

# INVESTIGATION ON THERMOMECHANICAL BEHAVIOR OF CuAlNi/POLYIMIDE BIMORPH

M.Tech. Thesis

By  
NARAYANE DHIRAJ CHINDHUJI

(Roll No. 1502103003)



DISCIPLINE OF MECHANICAL ENGINEERING

**INDIAN INSTITUTE OF TECHNOLOGY INDORE**

JUNE 2017

**INVESTIGATION ON  
THERMOMECHANICAL  
BEHAVIOR OF CuAlNi/POLYIMIDE  
BIMORPH**

**A THESIS**

*Submitted in partial fulfillment of the  
requirements for the award of the degree*

*of*  
**Master of Technology**

*by*  
**NARAYANE DHIRAJ CHINDHUJI**  
*(Roll No. 1502103003)*



**DISCIPLINE OF MECHANICAL ENGINEERING  
INDIAN INSTITUTE OF TECHNOLOGY  
INDORE**

**JUNE 2017**



# INDIAN INSTITUTE OF TECHNOLOGY INDORE

## CANDIDATE'S DECLARATION

I hereby certify that the work which is being presented in the thesis entitled **INVESTIGATION ON THERMOMECHANICAL BEHAVIOR OF CuAlNi/POLYIMIDE BIMORPH** in the partial fulfillment of the requirements for the award of the degree of **MASTER OF TECHNOLOGY** and submitted in the **DISCIPLINE OF MECHANICAL ENGINEERING, Indian Institute of Technology Indore**, is an authentic record of my own work carried out during the time period from July 2015 to June 2017 under the supervision of Dr. I. A. Palani, Associate Professor, Mechatronics and Instrumentation lab, Discipline Mechanical Engineering and Dr. B. K. Lad, Associate Professor, Industrial Engineering Research group, Discipline of Mechanical Engineering.

The matter presented in this thesis has not been submitted by me for the award of any other degree of this or any other institute.

(**NARAYANE DHIRAJ CHINDHUJI**)

-----  
This is to certify that the above statement made by the candidate is correct to the best of our knowledge.

(**Dr. I. A. Palani**)

(**Dr. B. K. Lad**)

-----  
**Narayane Dhiraj Chindhuji** has successfully given his/her M.Tech. Oral Examination held on.....

Signature(s) of Supervisor(s) of M.Tech. thesis

Date:

DPGC Convener,

Date:

Signature of PSPC Member 1

Date:

Signature of PSPC Member 2

Date:



# Acknowledgement

I take this opportunity to express my deep sense of respect and gratitude for, Dr. I.A. Palani, for believing in me to carry out this work under his supervision. His constant encouragement, friendly interactions, and constructive support have enabled this work to achieve its present form. His innovative perspective towards things and his continuous pursuit for perfection has had a profound effect on me and has transformed me majorly. I feel greatly privileged to be one of his students.

I am grateful to Dr. B.K. Lad, for his every-ready support and personal attention even in the busiest of his schedule. Discussions with him have been extremely knowledgeable and have significantly shaped this thesis.

I am thankful to IIT Indore for giving me an opportunity to carry out the research work and providing all the facilities. Very special thanks to Prof. Pradeep Mathur, Director, IIT Indore, for supporting and providing us facilities to perform my work smoothly here.

I am extremely thankful to Mr. Akash K. for guiding me and helping me out from the very first day I joined this project. I would also like to express my thanks to all members of Opto-Mechatronics group for their moral support and the friendly nature we have created in our lab.

Lastly, but undoubtedly the most valued, gratitude is expressed for my parents and my entire family for letting me choose my dreams and supporting me endlessly. Your un-matched support made this work possible.

Narayane Dhiraj Chindhuji

*Dedicated to my Guide –*

*my mother,*

*my father,*

*my family,*

*my teacher,*

*and my friends*

# Abstract

Thin film deposition of various shape memory alloys (SMA) on different substrates using different deposition techniques is being studied to get two-way shape memory effect for micro-actuator applications. The ability of SMA to generate sufficiently large amount of forces, large strain recovery makes SMA a prime member for its use in micro-actuator applications. However, low actuation frequency of around 1Hz and low transformation temperature under 100 °C makes commercially used NiTi SMA unsuitable for its use in high temperature situations. The transformation temperature and frequency of actuation can be increased to some extent by the addition of Cu as a ternary element in NiTi SMA.

As Cu-based SMAs are well known for its high transformation temperature and high frequency of actuation, CuAlNi SMA is selected for this research work. In this work, the thermo-mechanical behaviour of electrically actuated CuAlNi/Polyimide SMA bimorph has been studied in detail with three different compositions of SMA which was deposited using thermal evaporation technique. Thermomechanical behaviour is studied when actuation voltage, actuation frequency and applied load at bimorph was changed. Certain key relationships between these parameters are determined through experimental study. The life cycle behaviour of CuAlNi/Polyimide bimorph as well as Mn added CuAlNi/Polyimide bimorph is also studied. It is found from the experiments that Mn addition in CuAlNi significantly increases the actuation properties and life of CuAlNi thin film as a result of grain refinement and improvement in the ductility of CuAlNi. To study the compositional, morphological, thermal and mechanical properties of these CuAlNi SMAs relevant techniques and instruments have been used. All the results from these sophisticated instruments and the results of actuation prove the improvement in the thermal-mechanical properties of CuAlNi SMA thin film with addition of Mn.

## LIST OF PUBLICATIONS

### JOURNAL PUBLICATION

K. Akash, Ashish K. Shukla, S. S. Mani Prabu, **Dhiraj C. Narayane**, S. Kanmanisubbu, I. A. Palani, “Parametric investigations to enhance the thermomechanical properties of CuAlNi shape memory alloy Bi-morph.” *Published in Journal of alloys and compounds, Elsevier, Volume 720, 5 October 2017, Pages 264–271*

### CONFERENCE PUBLICATIONS

Akash K., Chandan K., Parikshit G., **Narayane Dhiraj C.**, Reena Disawal, B. K. Lad, Vipul Singh, Palani I. A. “Investigations on transformer oil temperature sensing using CuAlNi/polyimide shape memory alloy composite film.” *Published in SPIE Proceedings Volume 10165: Behavior and Mechanics of Multifunctional Materials and Composites 2017.*

Akash.K, Ashish Shukla, **Narayane Dhiraj Chindhuji**, Mani Prabu S S, Palani I A. “Thermo-mechanical Analysis of CuAlNi/Polyimide Composite film” *International Conference on Design and Manufacturing (IConDM 2016) at IITDM Kancheepuram, Chennai. Paper accepted & it is under the process of publication in IEEE Xplore.*

**Narayane Dhiraj Chindhuji**, Akash K,Vijay Choyal, Manikandan M, Lad.B.K, Palani.I.A., “Investigation on actuation behavior and life cycle behavior of CuAlNi/Polyimide shape memory alloy composite film.” *Paper accepted for ISSS international conference 2017 at IISc Bangalore.*

# TABLE OF CONTENTS

<b>Acknowledgement</b> .....	<b>i</b>
<b>Abstract</b> .....	<b>iii</b>
<b>LIST OF PUBLICATIONS</b> .....	<b>iv</b>
<b>LIST OF FIGURES</b> .....	<b>3</b>
<b>Chapter 1 Introduction</b> .....	<b>1</b>
1.1 Shape Memory Alloys .....	1
1.2 Shape memory effect.....	1
1.3 Cyclic behavior .....	4
1.4 Shape memory materials.....	5
1.5 Shape memory ally composites .....	6
1.6 Thermomechanical behavior .....	7
1.7 Research gap.....	9
1.8 Motivation .....	9
1.9 Research Objectives.....	11
1.9.1 Overall Objective.....	11
1.9.2 Intermediate Objective .....	11
<b>Chapter 2 Experimental Procedure</b> .....	<b>12</b>
2.1 Thermal Evaporation .....	12
2.2 Pre straining of polyimide substrate.....	14
2.3 Thermomechanical analysis setup.....	16
2.4 Tensile testing.....	17
2.5 Structural, morphological, thermal analysis .....	17
<b>Chapter 3 Thermo-mechanical behavior of CuAlNi/Polyimide shape memory alloy bimorph with Joule heating</b> .....	<b>19</b>
3.1 Selection of composition of CuAlNi SMA.....	19
3.1.2 Thickness measurement .....	19
3.2 Selection of thickness of polyimide .....	20
3.2.1 Voltage Vs displacement relationship .....	21
<b>Chapter 4 Thermo-mechanical behavior of CuAlNi/Polyimide SMA bimorph with changed composition and effect of Mn addition into CuAlNi SMA</b> .....	<b>26</b>
4.1 Morphological, Structural and Thermal analysis .....	26
4.1.1 Morphological, compositional analysis.....	26
4.1.2 Structural analysis.....	28

4.1.3 Thermal analysis.....	29
4.2 Tensile test.....	31
4.2.1 Comparison between Bimorphs and bare polyimide tensile test results:.	32
4.2.2 Comparison between CuAlNi/PI and CuAlNiMn/PI bimorphs tensile test results:.....	32
4.3 Thermomechanical Analysis .....	33
4.3.1 Load 30 mg.....	33
4.3.2 Load 45 mg.....	35
4.3.3 Load 60 mg.....	37
4.3.4 Maximum Displacement .....	38
4.3.5 Discussion.....	40
<b>Chapter 5 Life cycle behavior of CuAlNi/PI and CuAlNiMn/PI bimorph .....</b>	<b>44</b>
5.1 Life cycle of CuAlNi/PI bimorph .....	44
5.2 Life cycle of CuAlNiMn/PI bimorph.....	46
5.3 Reliability results:.....	49
<b>Chapter 6 Conclusion and future scope.....</b>	<b>51</b>
<b>Chapter 7 Bibliography .....</b>	<b>53</b>

## LIST OF FIGURES

Figure 1 (a) Observation of the response of a folded SMA sheet as it is heated. (b) Sectional view of a heated SMA folded sheet transmitting force to the blue structure. (c) The folded SMA sheet is connected to a structure to transmit the generated force (d) the configuration referred for linear motion	1
Figure 2 Schematic of phase transformation in shape memory alloys.	2
Figure 3 Various elements of shape memory alloy.	5
Figure 4 Polymer matrix reinforced with smart SMA and Bio inspired turtle robot embedded with SMA composite as actuators.	6
Figure 5 Micro-flapper aerial robot used SMA bimorph to flap the wings. Images are taken from research paper of Ishida A, Sato M (2008) and Ishida A (2015	7
Figure 6 Applications of SMA/Polyimide bimorph	10
Figure 7 (a) Image of thermal evaporation unit (b) Schematic of assembly of parts inside the glass vaccum chamber (c) Image of assembly of parts inside the glass vaccum chamber.	13
Figure 8 Graph showing the different transformation temperatures, phase change and shape memory effect exhibited by sample developed without any post-processing.	14
Figure 9 Images showing the steps involved in the development of bi-morphs and the shape memory effect exhibited by the bi-morphs	15
Figure 10 Images showing the pictures of (a) thermal evaporation setup (b) the developed bi-morph (c) the bi-morph cut into small samples for electrical actuation (d) block diagram of the electrical actuation setup.	16
Figure 11 (a) Image of the developed tensile testing equipment (b) Image of the clamp utilized for the testing process.	17
Figure 12 Different kind of tools used for the material characterization.	18
Figure 13 Thickness measurement using optical roughness profilometer.	20
Figure 14 Actuation experimentation for polyimide thickness selection	20
Figure 15 Maximum possible displacement for composite film without load.	21
Figure 16 Results for Time vs Displacement with 30 mg load at free end of bimorph	24
Figure 17 FE-SEM images for both CuAlNi and CuAlNiMn samples	26
Figure 18 EDS compositional results for CuAlNi and CuAlNiMn SMA.	27
Figure 19 XRD analysis showing the origination of martensite peaks in the bi-morphs.	28
Figure 20: Differential Scanning calorimetry analysis showing the transformation temperatures.	29
Figure 21 Thermal imaging of CuAlNi/Polyimide and CuAlNiMn/Polyimide bimorphs and its result.	30
Figure 22 Thermogravimetric analysis for bare polyimide, CuAlNi/PI and CuAlNiMn/PI bimorphs.	31
Figure 23 Comparison between stress-strain curve of polyimide and SMA bimorphs	31
Figure 24 Closer view of stress-strain curve upto early 1.4% strain	32
Figure 25 Electrical actuation results with 30 mg load at different voltages of 1 V, 1.5 V and 2 V (a) CuAlNi/Polyimide at 0.5 Hz (b) CuAlNiMn/polyimide at 0.5 Hz (c) CuAlNi/Polyimide at 0.33 Hz (d) CuAlNiMn/polyimide at 0.33 Hz (e) CuAlNi/Polyimide at 0.25 Hz	34

Figure 26 Electrical actuation results with 30 mg load at different voltages of 1 V, 1.5 V and 2 V (a) CuAlNi/Polyimide at 0.5 Hz (b) CuAlNiMn/polyimide at 0.5 Hz (c) CuAlNi/Polyimide at 0.33 Hz (d) CuAlNiMn/polyimide at 0.33 Hz (e) CuAlNi/Polyimide	36
Figure 27 Electrical actuation results with 60 mg load at different voltages of 1 V, 1.5 V and 2 V (a) CuAlNi/Polyimide at 0.5 Hz (b) CuAlNiMn/polyimide at 0.5 Hz (c) CuAlNi/Polyimide at 0.33 Hz (d) CuAlNiMn/polyimide at 0.33 Hz (e) CuAlNi/Polyimide at 0.25 Hz	37
Figure 28 Electrical actuation results comparing the maximum displacement of CuAlNi/polyimide and CuAlNiMn/polyimide samples at varying load and varying voltages. (a) 1 V, 30 mg (b) 1 V, 45 mg (c) 1 V, 60 (d) 1.5 V , 30 mg (e) 1.5 V, 45 mg (f) 1.5 V, 60 mg	40
Figure 29 Life cycle behavior of CuAlNi/PI bimorph	45
Figure 30 Digital microscopic image of deposited sample before actuation, Digital microscopic image of failed component after actuation.	46
Figure 31 Life cycle of CuAlNiMn bimorph	47
Figure 32 Digital microscopic image of deposited sample before actuation, Digital microscopic image of failed component after actuation.	48
Figure 33 Repeatability in Life cycle behaviour experimental result	48
Figure 34 Reliability vs Time relationship for CuAlNiMn/PI bimorph	49
Figure 35 Reliability vs Time relationship for CuAlNi/PI bimorph	50
Figure 36 Proposed design of the aerial robot with SMA bi-morph	52

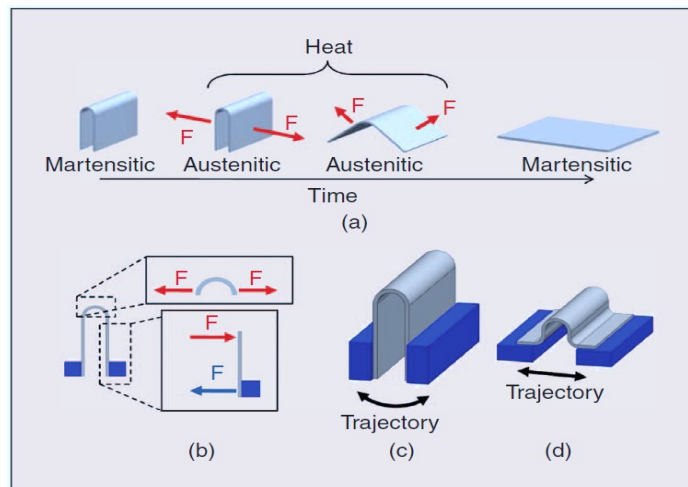
## LIST OF TABLES

Table 1 Parameters used for the deposition process .....	14
Table 2 Composition of each element in terms of weight. ....	27
Table 3 Life cycle data for CuAlNi/PI bimorph .....	45
Table 4 Life cycle data for CuAlNi/PI bimorph .....	47

# Chapter 1 Introduction

## 1.1 Shape Memory Alloys

Shape memory alloys are a group of smart materials that exhibit exceptional mechanical and thermal responses. Shape Memory Alloys (SMAs) have the ability to recover previously applied strains on the application of heat. As such, the alloys are able to recover their original geometry and such shape change that has led to development of substantial applications[1]. The functional properties of the SMAs, such as shape memory effect (SME), super-elasticity and the two-way shape memory effect (TWSME), are the result of a martensitic phase transformation that occurs between the austenite phase and the martensite phase[2,3]. Evidence of the martensitic transformation was first obtained by Otsuka *et. Al* who unambiguously demonstrated a correspondence between the shape memory effect and the thermo-elastic martensitic transformation in Cu-Al-Ni alloy[4].



**Figure 1 (a) Observation of the response of a folded SMA sheet as it is heated. (b) Sectional view of a heated SMA folded sheet transmitting force to the blue structure. (c) The folded SMA sheet is connected to a structure to transmit the generated force (d) the configuration referred for linear motion**

## 1.2 Shape memory effect

SMAs have two phases, each with a different crystal structure and therefore different properties. One is the high temperature phase called austenite (A) which generally has cubic structure and the other is the low temperature phase called martensite (M) which has different

Crystal structures as tetragonal, orthorhombic or monoclinic. The transformation from one structure to the other does not occur by diffusion of atoms, but rather by shear lattice distortion, named martensitic transformation. Each martensitic crystal formed can have a different orientation direction, called a variant. The assembly of martensitic variants can exist in two forms: twinned martensite (Mt), which is formed by a combination of “self-accommodated” martensitic variants, and detwinned or reoriented martensite in which a specific variant is dominant (Md). The reversible phase transformation from austenite (parent phase) to martensite (product phase) and vice versa forms the basis for the unique behaviour of SMAs[5–7].

Forward transformation occurs upon cooling in the absence of an applied load as the crystal structure changes from austenite to martensite. This

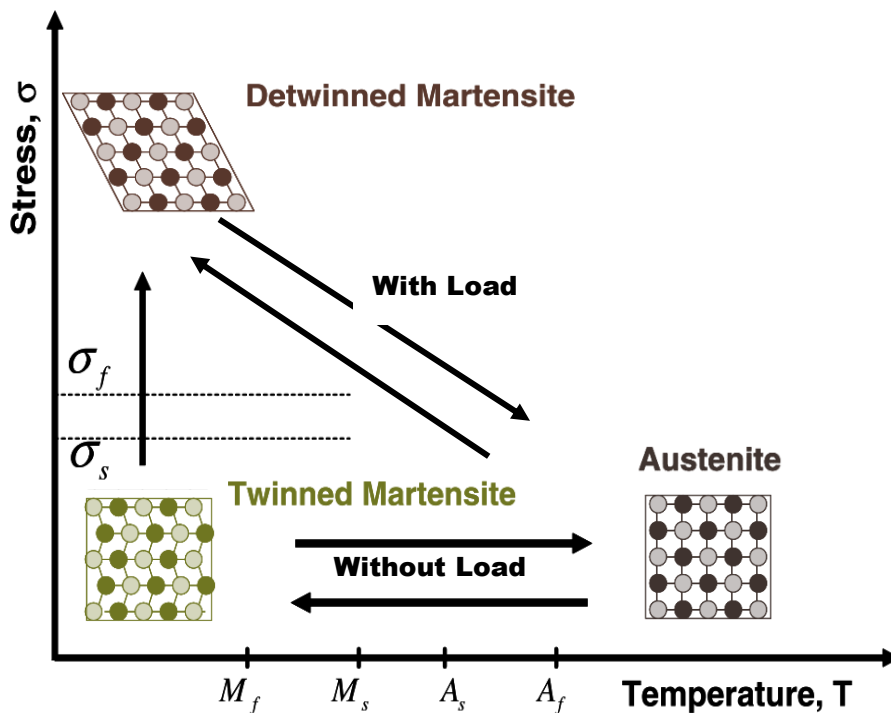


Figure 2 Schematic of phase transformation in shape memory alloys.

results in the formation of several martensitic variants as mentioned above. The arrangement of variants occurs such that the average macroscopic shape change is negligible, resulting in twinned martensite. The transformation during heating as the phase changes from martensite to austenite is termed as reverse transformation[8,9].

There are four characteristic temperatures associated with the phase transformation. During the forward transformation, austenite, under zero load,

begins to transform to twinned martensite at the martensitic start temperature ( $M_s$ ) and completes transformation to martensite at the martensitic finish temperature ( $M_f$ ). At this stage, the transformation is complete and the material is fully in the twinned martensitic phase. Similarly, during heating, the reverse transformation initiates at the austenitic start temperature ( $A_s$ ) and the transformation is completed at the austenitic finish temperature ( $A_f$ ).

As mechanical load is applied to the material, in the low temperature twinned martensitic phase, to detwin the martensite by reorienting a certain number of variants. The detwinning process results in a macroscopic shape change, where the deformed configuration is retained when the load is released. A subsequent heating of the SMA to a temperature above  $A_f$  will result in a reverse phase transformation (from detwinned martensite to austenite) and will lead to complete shape recovery[10,11]. Cooling back to a temperature below  $M_f$  (forward transformation) leads to the formation of twinned martensite again with no associated shape change observed. The process described above is referred to as the Shape Memory Effect (SME). The load applied must be sufficiently large to start the detwinning process. The minimum stress required for detwinning initiation is termed the detwinning start stress ( $\sigma_s$ ). Sufficiently, high load levels will result in complete detwinning of martensite where the corresponding stress level is called the detwinning finish stress ( $\sigma_f$ )[1]. When the material is cooled with a mechanical load greater than  $\sigma_s$  applied in the austenitic phase, the phase transformation will result in the direct formation of detwinned martensite, producing a shape change. Reheating the material will result in shape recovery while the load is still applied. A schematic of the above-described loading path shown in figure (2). Recognizing that the forward and reverse transformations occur over a range of temperatures ( $M_s$  to  $M_f$ ,  $A_s$  to  $A_f$ ) for a given SMA composition, we can construct transformation regions in the stress-temperature space. The transformation temperatures strongly depend on the magnitude of the applied load, with higher values of applied load leading to higher transformation temperatures[12,13].

### 1.3 Cyclic behavior

SMA can exhibit repeatable shape changes under no applied mechanical loading when subjected to a cyclic thermal load. This behaviour is termed as two-way shape memory effect (TWSME). The TWSME can be observed in a SMA material which has undergone repeated thermo-mechanical cycling along a specific loading path (training). Repetition along a loading path for a large number of cycles can induce changes in the microstructure, which causes macroscopically observable permanent changes in the material behaviour[14–17]. Training an SMA refers to a process of repeatedly loading the material following a cyclic thermo-mechanical loading path until the hysteretic response of the material stabilizes and the inelastic strain saturates. Let us consider the case of cyclic thermal loading of an SMA specimen under a constant applied stress. During the first thermal cycle, only a partial recovery of the strain generated during cooling is observed upon heating with some permanent (irrecoverable or plastic) strain generated during the cycle[18,19]. A small, permanent strain remains after each thermal cycle is completed. The additional permanent strain associated with each consecutive cycle begins to gradually decrease until it practically ceases to further accumulate. A similar behaviour can be noticed in the case of mechanically cycling an SMA repeatedly in its pseudoelastic regime, until saturation takes place. The TWSME behaviour can also be achieved by adopting different training sequences. A more recent technique that leads to TWSME deals with aging the material under stress in the martensitic state[20–22].

TWSME is a result of defects introduced during training. These permanent defects create a residual internal stress state, thereby facilitating the formation of preferred martensitic variants when the SMA is cooled in the absence of external loads. If the internal stress state is modified for any reason (e.g., aging at high temperature or mechanical overload), the TWSME will be perturbed.

## 1.4 Shape memory materials

Nickel-Titanium (Nitinol, NiTi) is the alloy primary used in applications. It exhibits strong SME, TWSME, and pseudoelastic behaviour under the right conditions, which makes this material ideal for a variety of applications. It also exhibits resistance to corrosion and is biocompatible, making it suitable for the use in biomedical applications. Compared to the less widely used alloys, the crystallography and thermomechanical response of NiTi are well understood,

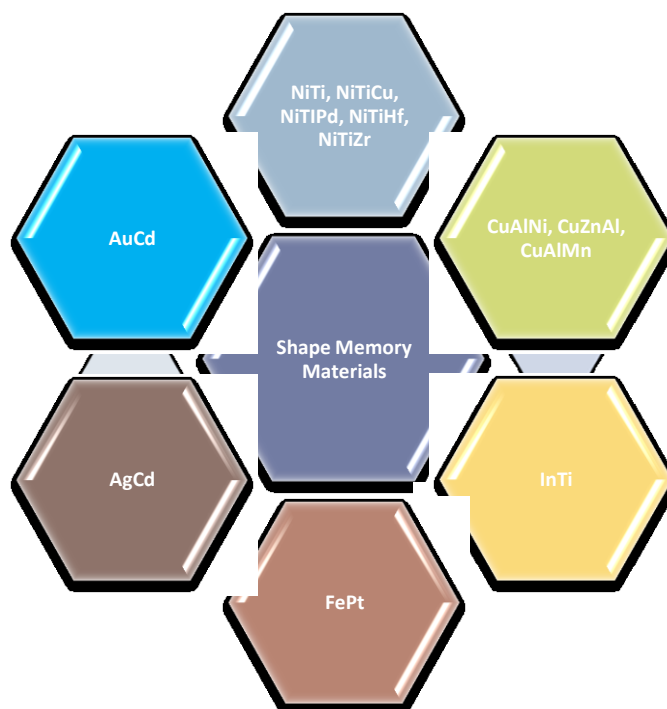


Figure 3 Various elements of shape memory alloy.

as the effects of heat treatment and the variation of transformation temperatures with changes in composition[23–27].

Copper based shape memory alloys can serve as an excellent alternative as they offer good electrical and thermal conductivity. Cu based SMAs have less hysteresis when compared to NiTi and the transformation temperatures are highly dependent on the composition (Chen, Liang, Fu, & Ren, 2005; Cingolani, Ahlers, & Sade, 1995). Apart from these properties, Cu based SMAs are highly energy efficient and they have excellent damping properties. The two most widely studied copper based SMAs are Cu-Zn and Cu-Al. CuZnAl alloys are very ductile and resistant to intergranular fractures. Actuation temperatures are below room temperature, but addition of Al from 5 wt% to 10 wt% increase transformation temperature to 100°C [32]. The

conventional development such as melt process has difficulties in maintaining the composition as zinc gets evaporated because of its low melting point. However this may not be the case when an alloy sputtering target is using for the deposition of thin film[33–36].

### 1.5 Shape memory alloy composites

Composite SMA Structures were first developed by Rogers (1991) where they embedded NiTi wires in a laminated polymer matrix composite (PMC)[37]. After that, there have been several reports on SMA composites leading to latest development by Ishida.A (2014), in which he has developed a NiTi/Polyimide bi-morph and explored its potential application as micro-flapper[38–41]. Further Kotnur(2014) has studied the influence of different parameters while developing NiTi/Polyimide composites through sputtering at low temperatures[42,43]. However the thermomechanical behavior of such films has not been studied in detail[44].

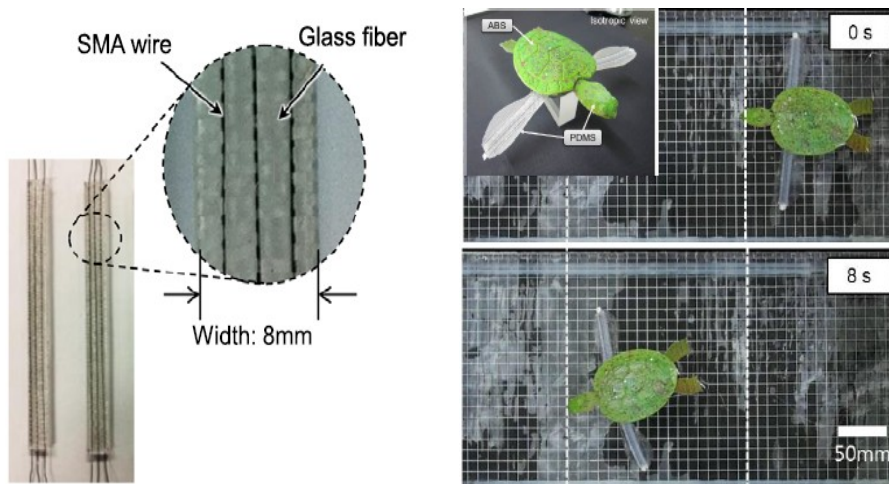


**Figure 4 Polymer matrix reinforced with smart SMA and Bio inspired turtle robot embedded with SMA composite as actuators.**

There are several reports on using NiTi, however other alternatives such as CuAlNi serves as an efficient and cost effective choice[10,45–48]. The primary limitation of CuAlNi shape memory alloy is its poor ductility. This leads to drastic decline in its cyclic behavior. This can be overlooked by using a pre-strained flexible substrate, which can assist during cyclic loading and unloading. Parameters such as composition, substrate thickness, and addition of Mn and Ti might result in better properties. However, the influence of

substrate temperature is an essential parameter which can be used to produce enhanced SMA films without altering the transition temperature.

The thermomechanical behaviour of shape memory alloy can be tuned by post processing techniques such as annealing and training. However, employing such techniques in thin films can be a tedious task. An alternative approach of developing the thin films on various substrate temperatures can be a utilized to improve the thermomechanical behaviour. The substrate temperature during deposition plays a vital role in the crystallinity of the

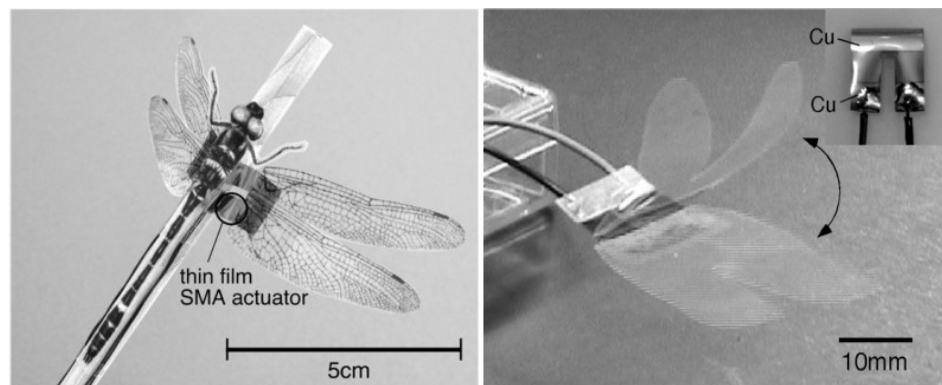


**Figure (5) Micro-flapper aerial robot used SMA bimorph to flap the wings. Images are taken from research paper of Ishida A, Sato M (2008) and Ishida A (2015)**

developed film. There have been several reports of deposition on heated substrates which facilitates in avoiding the high temperature annealing required after deposition[15,49]. High temperature surfaces can be effective place for nucleation and further it can improve the diffusion process leading to enhanced crystallization. Developing CuAlNi shape memory alloys on different substrate temperatures benefits in overcoming the cyclic behavioral issues encountered after the development process.

## **1.6 Thermomechanical behavior**

Since SMAs are widely preferred for actuation and sensing applications that require multiple cycles, it is important to analyse the cyclic effects of transformation induced fatigue. The fatigue behaviour of SMAs depends on the material processing (fabrication process, heat treatment, etc.), the type of loading conditions (applied stress, strain, temperature variations, environment, etc.), and transformation induced microstructural modifications (e.g., defects

on grain boundaries due to strain incompatibilities). In most SMA applications, a large number of transformation cycles are induced by repeating a loading path that exhibits thermally induced phase transformation under applied load. As discussed in the previous section, repeated loading along a thermomechanical path causes gradual microstructural changes. These changes cause the degradation of the SMA behaviour leading to low cycle fatigue as opposed to high cycle fatigue most commonly observed in loading paths operating in a purely elastic regime of a material. This section will provide a brief review of mechanically and thermally induced transformation fatigue behaviour of SMAs.

Mechanically induced fatigue behavior of SMAs is typically examined by performing rotating bending tests or by mechanically cycling the material on the load frame between two stress or strain levels along a given loading path [18, 21]. Such mechanical cycling can be performed to induce a complete transformation (i.e., cycled between complete austenite and martensite phase) or partial transformation (cycling between states where one or both end limits are not purely martensite or austenite but a mixture). If the deformation or stress level applied to the SMA specimen remains within the elastic regime, this can lead to fatigue life as high as  $\sim 10^7$  cycles. However, in some cases, the material can be taken through detwinning or stress induced martensitic transformation by applying sufficiently high load levels. In such cases, the material fails considerably earlier in what is termed “transformation-induced low cycle fatigue,” with a fatigue life of the order of thousands of cycles [22, 23]. Similar to mechanically induced transformation fatigue, thermally-induced transformation fatigue behavior of SMAs is extremely important to study for actuation applications. Fatigue life for SMAs undergoing thermally-induced transformation cycles under applied load is dictated by the amount of transformation strain allowed to occur (partial or complete transformation) as well as the stress level under which the material is cycled. The amount of cyclic transformation strain allowed in the material can significantly affect the number of cycles to failure [24] under conditions of partial transformation.

## 1.7 Research gap

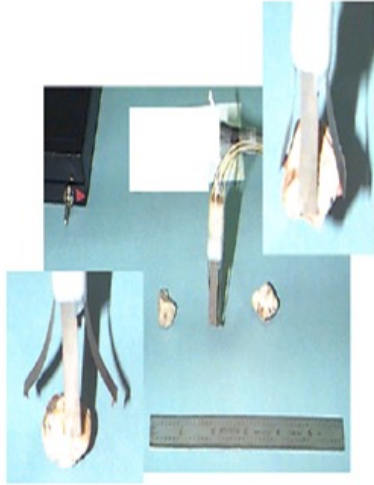
Literature review shows some gaps over which work is done here. There are several reports on bulk SMAs but are very few with SMA bimorphs. Bulk NiTi is immensely studied over the years. In 1998, 2005, and 2008 a Japanese researcher A Ishida published the work on NiTi/Polyimide bimorph. But there are no reports on Cu based SMA/Polyimide bimorph. Also there are no reports on life cycle behaviour, Adhesion of SMA thin film to polyimide, thermomechanical behaviour with different compositions of SMA for any SMA/Polyimide bimorphs.

## 1.8 Motivation

Smart materials have received increased demand in recent years because of their immense potential in revolutionizing engineering applications. Among the smart materials currently in research, Shape memory alloys predominant for the reason that large recoverable strains occur within it due to crystallographic transformation. The cyclic behaviour of SMA thin film bimorphs can be a better alternative to other materials for micro-actuator applications due its energy efficiency, large work to volume ratio, moderate force with long stroke length on actuation. CuAlNi SMA can be a good alternative to NiTi because some of its better qualities over NiTi such as its cost effectiveness, low fabrication cost, ease in fabrication, low hysteresis, high damping capacity, thermal & electrical conductivities, high transformation temperature, high actuation frequency etc. The prime drawback of CuAlNi SMA is its poor ductility and relatively low recoverable strain compare to NiTi. Its brittleness leads early life failure during actuation when actuate it longer number of cycles. On improving mechanical properties its life can be improved and make it a better alternative to NiTi.

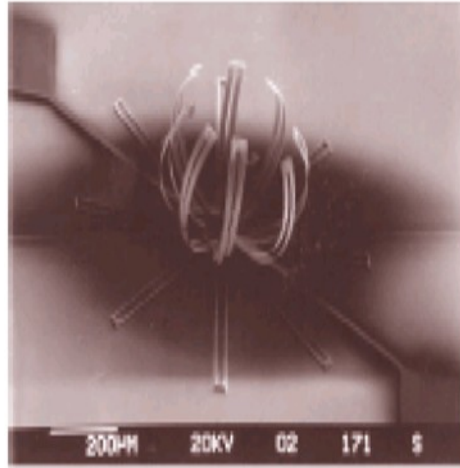
SMA actuators can be used in MEMS devices such as micro-pump, micro-wraper, tiny heart pumping device etc. Fig. (6) shows such devices. Fig. (6) (a) shows gripper which can be used in the electronic assemblies of delicate parts and which are not accessible. (b) shows micro-wraper which is used in

bio-medical devices for removing tumours in surgery. (c) shows the micro-pump and (d) shows the positioning platform which is of two degrees of freedom and it can be fabricated easily with SMA bimorphs.



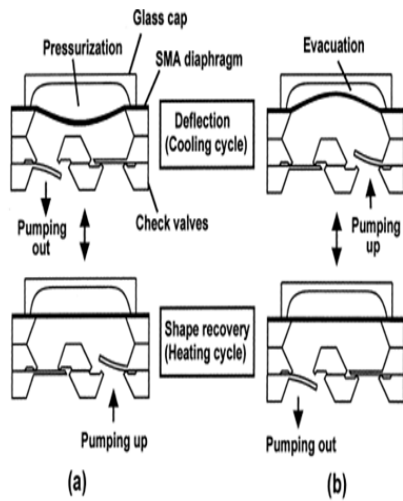
**Four-finger gripper**  
Mohsen Shahinpur et al.(2004)

(a)



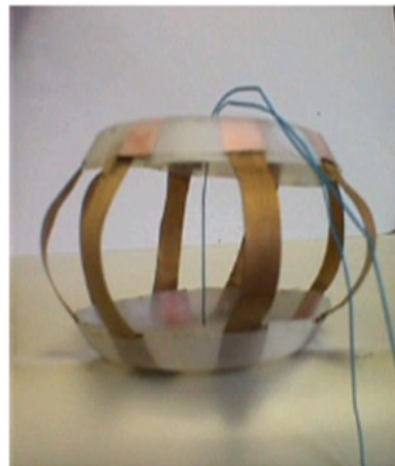
**Microwrapper**  
Gill et.al.

(b)



**SMA micropump (a) Suction mode (b) Pumping mode.**  
*Benard WL et .Al (1997)*

(c)



**Platform actuator** Mohsen Shahinpur et al.(2004)

(d)

**Figure 6 Applications of SMA/Polyimide bimorph**

## **1.9 Research Objectives**

### ***1.9.1 Overall Objective***

The overall objective of this thesis is to “Investigate the thermo-mechanical behavior of CuAlNi/Polyimide bimorph.”

### ***1.9.2 Intermediate Objective***

- I. To develop a test setup for performing thermomechanical analysis of CuAlNi/Polyimide shape memory alloy.”
- II. To gain actuation using DC power supply as the heat source.
- III. Development of CuAlNi/Polyimide bimorphs with different substrate thickness and different composition of SMA.
- IV. Improvement of mechanical properties of CuAlNi SMA with the addition of alloying element.
- V. To optimize operating parameters like applied mechanical load, actuation voltage, actuation frequency and study the effect of these parameters on actuation behavior of bimorph.
- VI. To get a comparison between actuation when done with a CuAlNi and with a addition of quaternary element.
- VII. Characterization of samples with various characterization techniques.
- VIII. Performing the experiments for life cycle behavior of SMA/Polyimide bimorphs and determination of reliability.

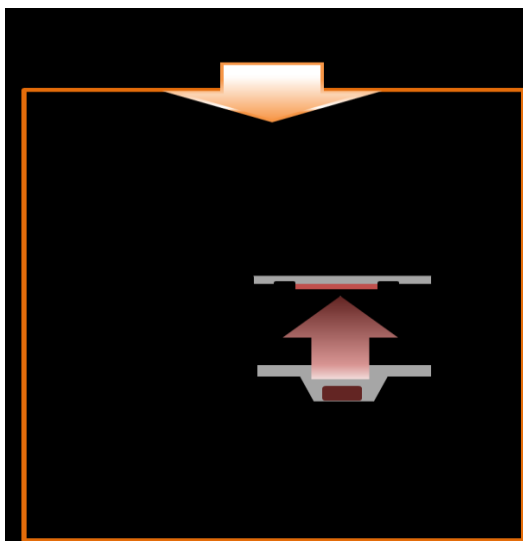
# Chapter 2 Experimental Procedure

The deposition was carried out by thermal evaporation technique. Thermal evaporation technique is considered to be one of the straight forward methods for developing thin film, where the material to deposited is placed in a boat. High current is supplied to the boat which will melt the material and then evaporate it. The normally used boat material is tungsten due its high melting point. The influence parameters of the deposition process include (i) the distance between the crucible (boat) and substrate (i) rate of deposition (iii) nature of the substrate. This chapter will discuss about the deposition process, pre-straining of polyimide and the thermomechanical behaviour setup used for the actuation studies.

## 2.1 Thermal Evaporation

Cu-Al-Ni/Polyimide bi-morphs have been developed through direct thermal evaporation method on flexible pre-strained Kapton polyimide sheet of different thickness. Table 1 shows the parameters used for developing SMA bi-morph. The raw materials were of 99.99% purity. The polyimide sheets were baked and cleaned before the deposition process. The sheets were cut into  $7 \times 7$  cm<sup>2</sup> pieces and were pre-strained and clamped to the substrate holder. The deposition processes was conducted in two steps (i) increase the temperature till the eutectoid point and allow the metals to be in completely molten state (ii) rapidly increasing the temperature which leads to the evaporation of the material. Figure 1 shows the block diagram of the deposition process. The same procedure was followed for development of films at different substrate temperatures.

(a)



(b)



(c)

Figure 7 (a) Image of thermal evaporation unit (b) Schematic of assembly of parts inside the glass vacuum chamber (c) Image of assembly of parts inside the glass vacuum chamber.

Table 1 Parameters used for the deposition process

Parameters	Value
Substrate Thickness of deposited film	Kapton Polyimide Sheet 50 $\mu\text{m}$ – 100 $\mu\text{m}$ 4 $\mu\text{m}$
Pellet Holder Distance between crucible and substrate	Tungsten crucible 15 cm
Current Metals Substrate heating	$\approx 120$ A Cu, Al, Ni, Mn Without Heating

## 2.2 Pre straining of polyimide substrate

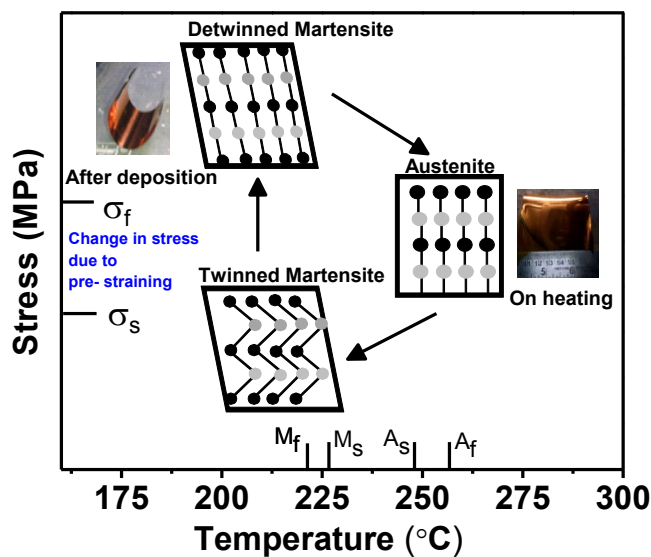
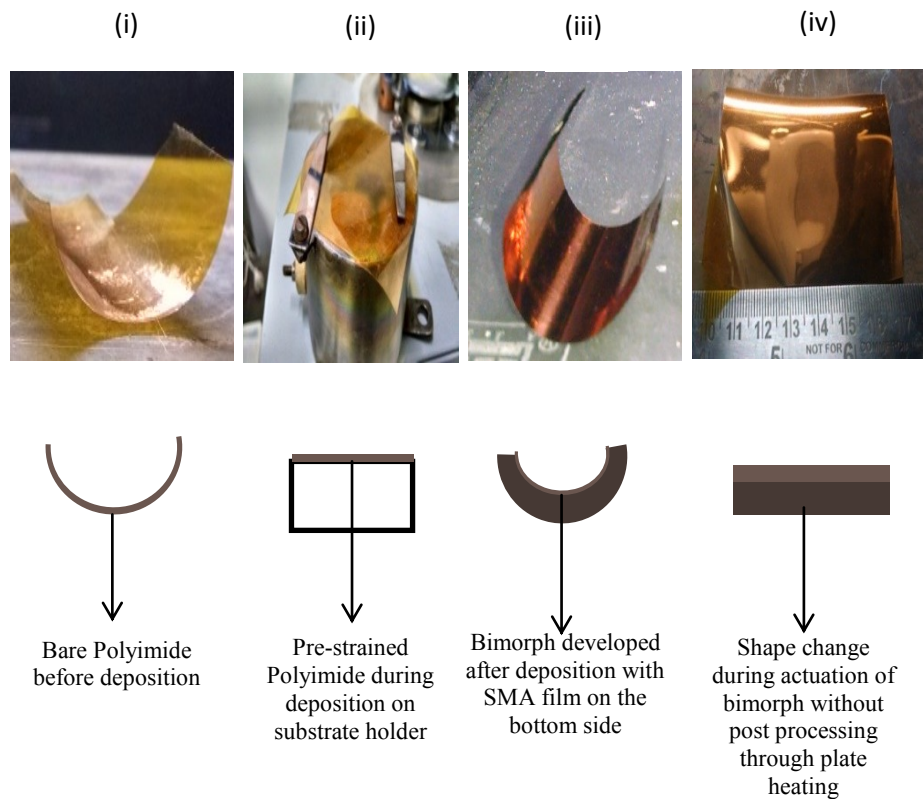


Figure 8 Graph showing the different transformation temperatures, phase change and shape memory effect exhibited by sample developed without any post-processing.

The developed bi-morphs displayed two-way shape memory effect without any post processing and training. Figure 8 explains the mechanism of shape memory effect achieved, phase change and the transformation temperature of the bi-morphs developed. This two-way behaviour is due to the pre-straining of the polyimide sheet during deposition. The pre-strained polyimide sheet

will act as the platform to initiate twinned martensite phase. Typically, an external stress is applied to the alloy, which will be recovered on the application of heat. However with the present method, the alloy can be deposited on the pre-strained flexible sheet which will induce the stress upon removal from the substrate holder. Upon removal, the developed bi-morph sheets exhibited two-way shape memory effect on the application of heat. To induce different shapes as required by the application, the pre-straining constraints should be different.

Figure 9 shows the images of the development process and the bi-morphs exhibiting the shape memory effect during heating and cooling. With thin films shape memory alloys, it becomes a tedious task to train the film after deposition. The method used in this research work can be utilized to achieve two-way effect. The developed films were characterized using scanning electron microscope, energy dispersive spectroscopy, adhesion tests, X-Ray diffraction and differential scanning calorimetry. Further the recovery ratio and the life cycle behavior of the bi-morphs are studied.



**Figure 9 Images showing the steps involved in the development of bi-morphs and the shape memory effect exhibited by the bi-morphs**

### 2.3 Thermomechanical analysis setup

To probe the suitability of the developed bimorph in MEMS microactuator application, electrical actuation setup was utilized as shown in figure 10(d). Life cycle of the bimorph has to be investigated thoroughly before considering it for potential applications. It consists of a K-type thermocouple, data acquisition system with 22 channels (Model: 34970 A, Agilent) and programmable power supply. The heating and cooling cycles were recorded by a laser displacement sensor (Model: HLG108-A-C5, Panasonic).

Different devices were used for the analysis. Figure 10(d) shows the life cycle analysis setup. Using the setup, three different frequencies of 0.25 Hz, 0.33 Hz and 0.5 Hz were exercised. In order to obtain the maximum displacement of the bimorph at different voltages. An actuation voltage of 2V and an actuation frequency of 0.5 Hz was chosen and fatigue life was tested and the results are

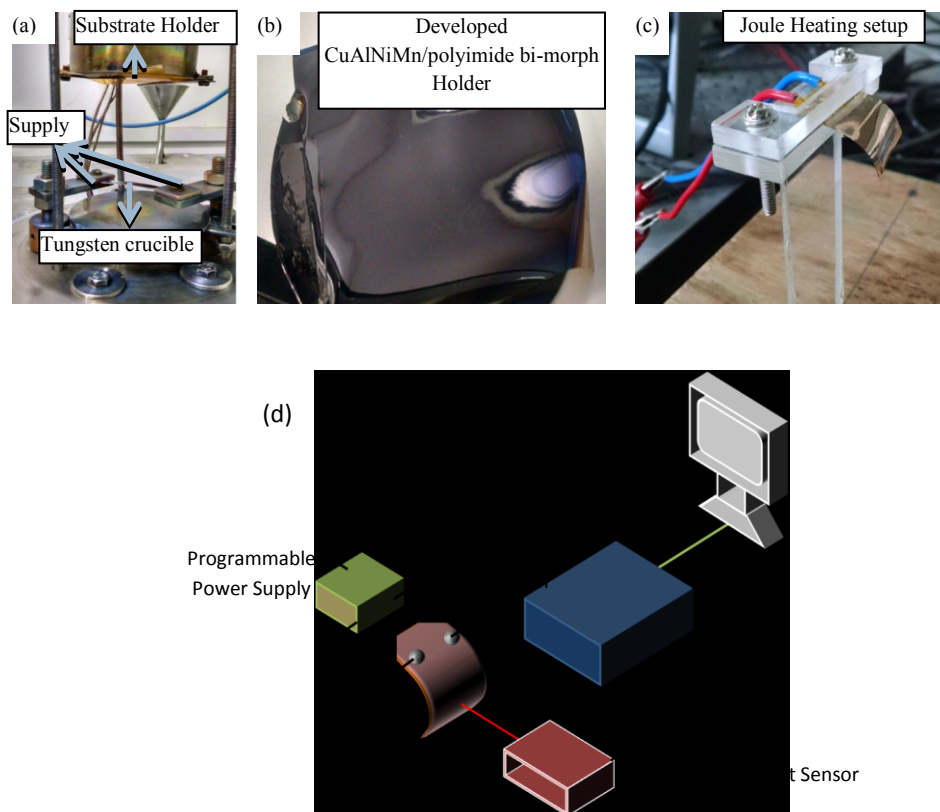


**Figure 10** Images showing the pictures of (a) thermal evaporation setup (b) the developed bi-morph (c) the bi-morph cut into small samples for electrical actuation (d) block diagram of the electrical actuation setup.

summarized.

## 2.4 Tensile testing

In order to analyze the stress-strain behavior of the developed bi-morphs, an in-house established tensile testing instrument was utilized. Fig. 11 (a) shows the images of the tensile testing equipment and 11 (b) shows the clamp design utilized for the testing process. The tensile testing equipment was employed with a commercially available load cell (Rudrra RS-302) of 5 kgf with sensitivity of 2 mV/V to measure the applied load. A stepper motor and low-pitch lead screw interfaced with arduino was utilized for smooth application of load. The clamps were specially designed to exert uniform tension throughout the bi-morph during operation. Table 1 shows the specifications of the tensile testing equipment.

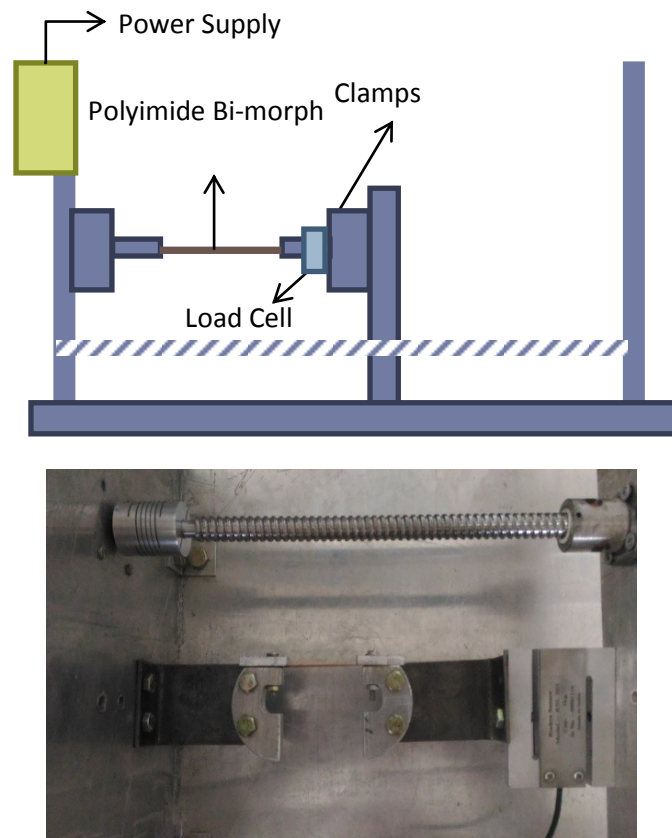
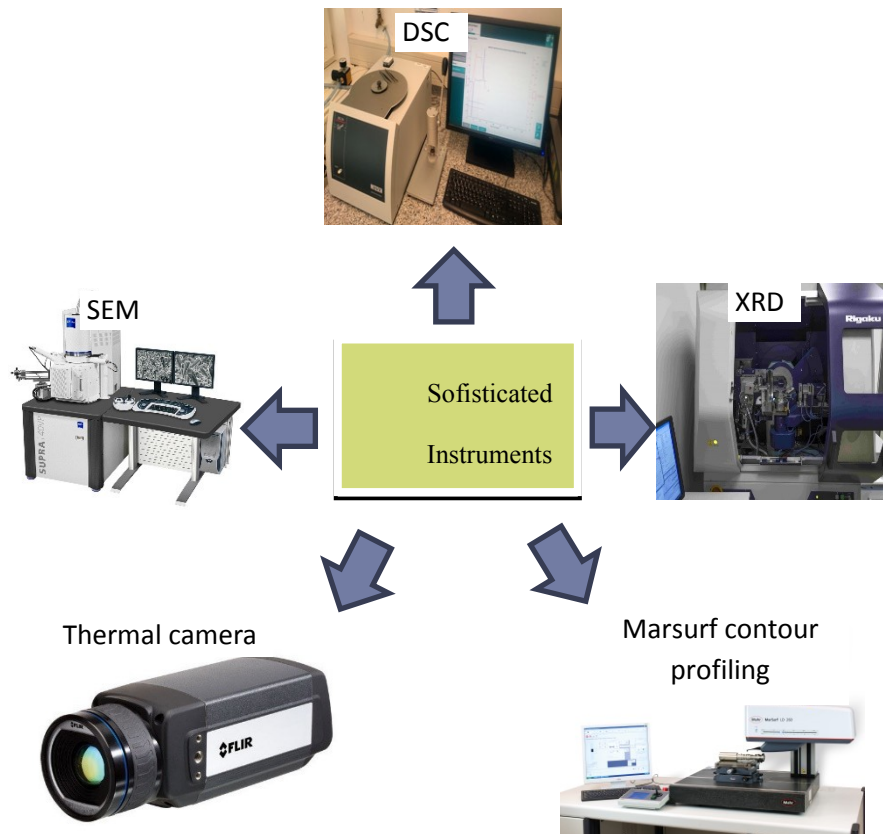


Figure 11 (a) Image of the developed tensile testing equipment (b) Image of the clamp utilized for the testing process.

## 2.5 Structural, morphological, thermal analysis

The scanning electron microscopic (FE-SEM) and energy dispersive x-ray analysis (EDX) were carried out by SUPRA55 Zeiss and XRD profiles

were recorded by RIGAKU SMARTLAB instrument using monochromatic Cu K $\alpha$  (1.541 Å) radiation. The thickness of the samples were measured using Marsurf LD 130 Roughness and Contour profile measurement. Further, the transformation temperatures of the bi-morphs were measured using differential scanning calorimetry (DSC – Netzch) and the analysis was extended by capturing thermal images from FLIR thermal camera. The adhesion test were carried out using scotch tape analysis.



**Figure 12** Different kind of tools used for the material characterization.

# Chapter 3 Thermo-mechanical behavior of CuAlNi/Polyimide shape memory alloy bimorph with Joule heating

## 3.1 Selection of composition of CuAlNi SMA

In this work an attempt has been made to study the actuation behavior of Cu-rich CuAlNi/polyimide SMA bimorph with varying composition of alloy. CuAlNi films with different combinations of composition was deposited on Kapton polyimide sheets by thermal evaporation technique, out of these few films were able to actuate considerably. A preliminary work was carried out with a SMA film with Cu-14.1 wt.% Al-3.2 wt.% Ni shape memory alloy (SMA) as it was able to actuate with maximum amount when put it on a hot plate. In this study, CuAlNi SMA thin film with mentioned composition was deposited on polyimide substrate with three different thickness i.e. 50 $\mu\text{m}$ , 75 $\mu\text{m}$  and 100 $\mu\text{m}$  on area of 70 $\times$ 70 mm<sup>2</sup>.

### 3.1.2 Thickness measurement

CuAlNi/Polyimide composite film was taken which was deposited partially i.e. half part deposited and other half undeposited to measure the thickness of CuAlNi SMA film on polyimide. Figure (13) shows the roughness profile of composite film. Abrupt change in the roughness profile is because of SMA film and maximum peak to valley value i.e. Rt can be considered as approximate thickness of SMA thin film and it comes out to be approximately 3.99  $\mu\text{m}$ .

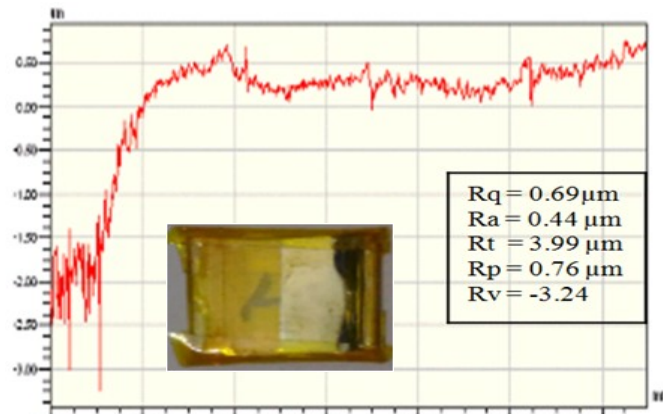


Figure 13 Thickness measurement using optical roughness profilometer.

### 3.2 Selection of thickness of polyimide

CuAlNi/Polyimide bimorph beam of area  $15 \times 15 \text{ mm}^2$  was chosen for the actuator. The film was actuated using electrical heating and the thermo-mechanical behavior of the developed sheets has been studied in detail. Actuation experiments were performed for all the three bimorphs with different polyimide thickness for the actuation voltages of 1V and 1.5V to determine the difference in actuation with three different polyimide thickness. All the three bimorphs are with same SMA composition & film thickness. Experiments were conducted for 10 cycles and at a frequency of 0.25 Hz for each sample and the load of 30 mg at the free end of bimorph.

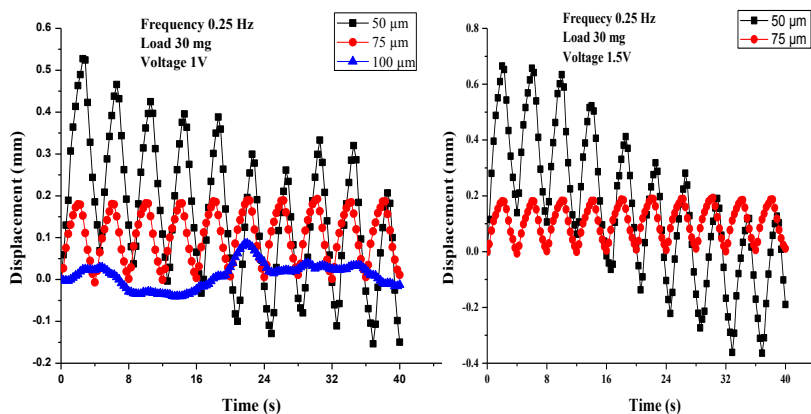


Figure 14 Actuation experimentation for polyimide thickness selection

Result in figure reveals the cyclic repeatability for the bimorph with 75  $\mu\text{m}$  polyimide thickness. For bimorph with 50  $\mu\text{m}$  polyimide thickness, displacement increased drastically but suddenly it starts to reduce after early

cycles and there is no repeatability in terms of initial and final position of the bimorph. For the bimorph with polyimide thickness 100  $\mu\text{m}$ , there is no evidence of any actuation. This is because the stiffness of a polyimide increases with the thickness and increase in stiffness causes reduction in deflection of the component with same amount of applied force considering same amount of force is generated by SMA film as composition and thickness of SMA film is same for all three bimorphs. Also, with increase in thickness or depth of the component the area moment of inertia increases drastically as it is directly proportional to cube of the thickness of component. And increase in area moment of inertia causes deflection to reduce drastically because deflection of a cantilever beam is inversely proportional to area moment of inertia. Hence, for the bimorph of polyimide thickness 100  $\mu\text{m}$ , it is difficult to find any deflection. With reference to above results, SMA bimorph with polyimide thickness of 75  $\mu\text{m}$  was chosen for further experimentation.

### 3.2.1 Voltage Vs displacement relationship

Experiments were performed at various voltages. It was observed that the amount of actuation displacement is a function of applied voltage as well as frequency of actuation of the film. CuAlNi/Polyimide composite film actuators at higher voltages show maximum linear displacement but found to be a very short life span, due to overheating.

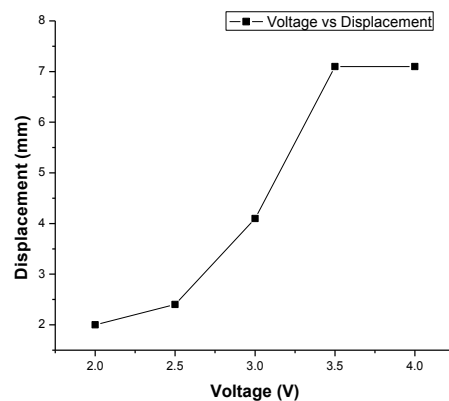
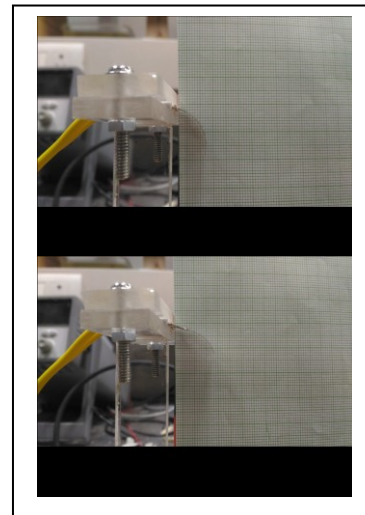


Figure 15 Maximum possible displacement for composite film without load.



In figure (15), we can see the relationship between voltage and displacement for heating duration of 8 seconds. Voltage vs displacement graph shows the maximum possible displacement of CuAlNi/Polyimide composite film for a particular voltage value. Voltage was applied to composite film continuously

for 8 seconds, actuation was seen for the duration of first 4 seconds of heating cycle. For the next 4 seconds, composite film was stagnant and there was no further actuation after first 4 seconds. Values of displacement for 2V, 2.5V, 3V, 3.5V and 4V are 2 mm, 2.4 mm, 4.1mm, 7.1 mm and 7.1 mm respectively. It is found that the displacement values for 3.5V and 4V are same i.e. 7.1 mm. This same value of displacement for both 3.5V and 4V shows the complete transformation of twinned martensite to austenite phase at these applied voltages for the duration of 4 seconds.

Therefore, the voltage of 3.5V is required for the CuAlNi SMA thin film to produce heat which would be sufficient to raise the temperature of SMA film to its austenite finish temperature ( $A_f$ ). Heating SMA above austenite finish temperature does not contribute to further shape recovery as the shape of deformed SMA only can be recovered in the temperature range of austenite start temperature ( $A_s$ ) to austenite finish temperature ( $A_f$ ). Displacement for the applied voltage of 4V is same as that of the displacement for 3.5V because overheating above  $A_f$  temperature with 4V does not recover any shape when  $A_f$  temperature is reached. Therefore the voltage of 3.5V and above will have the same displacement value and heating SMA by applying voltage above 3.5V may damage or burn the film by overheating, this can also be seen with the results shown in figure (16) for 30 mg load applied at the free end of composite film and actuation frequency of 0.25 Hz where displacement for 3.5V and 4V is same but the film got damaged due to overheating and it could survive only upto 3 cycles for voltage value of 4V. The Voltage vs displacement results can be observed to conclude that 3.5V is optimum voltage for CuAlNi SMA thin film to reach  $A_f$  temperature and get the maximum possible displacement.

For CuAlNi/Polyimide composite film to work as an actuator or small gripper in assembly of electronic parts, it has to move certain weight. For this reason beam had been loaded. Trial was taken to move the maximum possible weight with the available actuator of 4  $\mu\text{m}$  thickness. It was found that the actuator could move maximum weight of 60 mg with this thickness of the film. It was also found that there is very less amount of displacement of the actuator for

the weight beyond 30 mg. Therefore, maximum weight that actuator can move with sufficient amount of displacement was chosen to be 30 mg and the experiments were performed for thermomechanical behaviour of CuAlNi/Polyimide composite film with the weight of 30 mg at the free end of film. In figure (16), thermo-mechanical behavior of CuAlNi/Polyimide composite film can be seen for 30 mg load attached at the free end of composite film.

Voltages for actuation are chosen from 2V to 4V for the reason that composite film does not actuate at voltages less than 2V because heat produced by these voltages is not sufficient to reach the phase transformation temperature of CuAlNi SMA and therefore there is no shape recovery due to heating at these applied voltages. Actuation experiments were performed for different voltages only up to 4V for the reason that there is no any improvement in the actuation of composite film for 4V compare to 3.5V. Also, it was found from the results that, for actuation voltage of 4V, the life of CuAlNi SMA/polyimide composite has been reduced. Actuation frequency of film was taken as 0.25 Hz for the reason that the higher frequency actuation does not show the considerable displacement. Further, it was found from the higher frequency actuation that the repeatability is an issue. From the number of experiments for different frequencies of 0.5 Hz, 0.33 Hz, 0.25 Hz, it was observed that lower frequency actuation always produces better results as compared to higher frequency actuation in terms of displacement and repeatability. Also, for high frequency actuation, CuAlNi SMA does not get sufficient time to heat up and to reach the complete phase transformation for a particular voltage. Therefore an optimum frequency of 0.25 Hz was used for actuation of the composite film. The results obtained had more displacement and better repeatability at this frequency compared to higher frequencies.

In figure (16), it is observed from the results that there is very minor actuation with 1V and 1.5V. Also for actuation voltages of 2V and 2.5V that there is no considerable improvement in the displacement when voltage was increased from 2V to 2.5V. For the voltage of 3V, there is rapid actuation compared to lesser voltages. It can be observed from the results, for actuation voltages of 2V, 2.5 V and 3V, the return stroke length is same as that of actuation stroke.

The composite film comes back to its initial position by the bias force of pre-stained polyimide during cooling cycle. It is observed for 3.5V and 4V that, composite film does not return back to its initial position on cooling cycles. Here, in this case the actuation rate increases with the applied actuation voltage which clearly observed from the results.

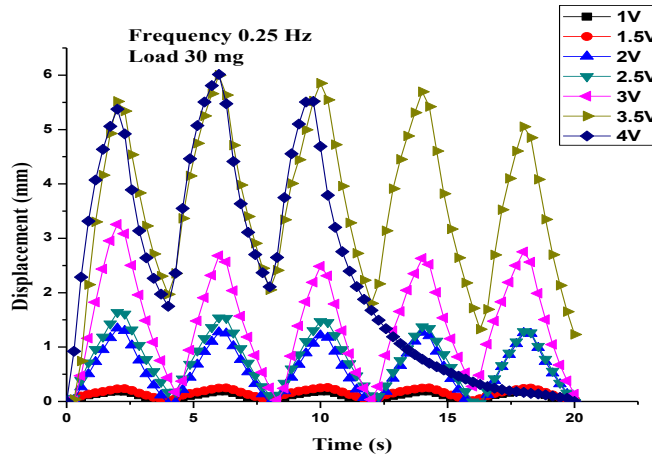


Figure 16 Results for Time vs Displacement with 30 mg load at free end of bimorph

With increase in voltage from 2.5V to 3V and 3V to 3.5V, there was rapid increase in displacement due to instant heating of CuAlNi SMA thin film on increasing the voltage which results into faster phase transformation. Therefore for the same heating duration, the displacement of composite film increases drastically with increase in the actuation voltage above 2.5V. As heating rate of CuAlNi SMA increases with applied actuation voltages, its cooling rate also increases due to large difference in the temperatures at the end of actuation and room temperature. Therefore, the span of displacement of composite film during return stroke was also increased with the voltages. For higher actuation voltages of 3.5V and 4V, composite film does not return back to its initial position during cooling as it requires more time to cover the long span which was created during actuation stroke due to heating with high voltage which results into rapid phase transformation. However, if more cooling time is provided during cooling cycle, the SMA film would come to its initial position.

Results for the voltage of 3.5V and 4V proved to be interesting, as the increase in voltage from 3.5V to 4V resulted in no change in the final displacement and

it is true for both without load and load of 30 mg at the free end of composite film. It is observed from the results of 30 mg load and the actuation voltages of 3.5V and 4V that there is rapid actuation for 4V due to rapid phase transformation as heating rate is more for the voltage of 4V compare to 3.5V. On observing the first heating cycle for 4V, it is seen that after achieving certain displacement rapidly by composite film its rate of increase in displacement reduced and becomes same as that of the displacement rate of 3.5V. Results for the voltages of 2V, 2.5V and 3V shows the partial solid state phase transformation or an intermediate bi-phase state of CuAlNi SMA thin film whereas the results for the voltage of 3.5V, 4V shows the complete solid state phase transformation. Result for the voltage of 4V shows the early failure of CuAlNi SMA thin film. This early life failure of CuAlNi SMA thin film is because of burning due to overheating at higher voltage.

# Chapter 4 Thermo-mechanical behavior of CuAlNi/Polyimide SMA bimorph with changed composition and effect of Mn addition into CuAlNi SMA

## 4.1 Morphological, Structural and Thermal analysis

### 4.1.1 Morphological, compositional analysis

To study the thermo-mechanical behaviour of CuAlNi thin film, its composition was changed. The scanning electron microscopic images for Mn added sample, present a smooth and uniform surface without any pores or cracks. The grain size

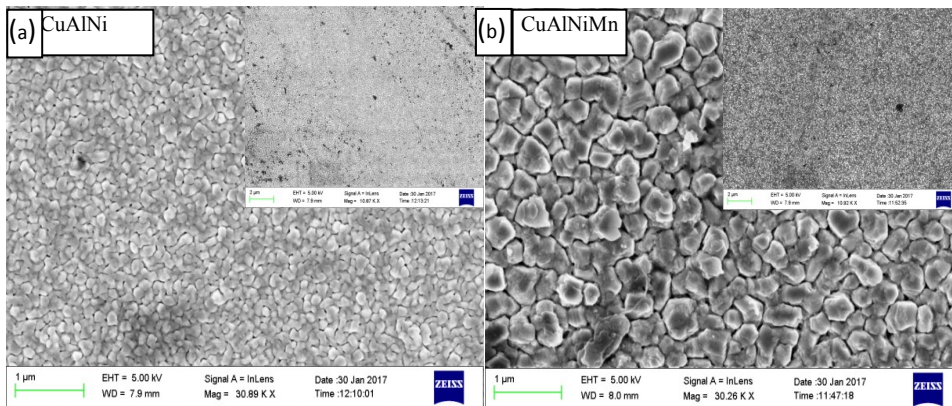


Figure 17 FE-SEM images for both CuAlNi and CuAlNiMn samples

was calculated to be less than 150 nm for samples developed without Mn. CuAlNi/polyimide samples exhibited distinct grain boundaries with closely packed grains. Fig. 17 (a) shows the surface morphology of CuAlNi/ polyimide bi-morph and Fig. 17 (b) shows the morphology of Mn added samples. The inset in Fig. 17 shows lower magnification image of the samples. It can be observed from the images, the grain size of samples developed with Mn was larger with approximately 300 nm to 350 nm, as measured using open source Image software. The samples with Mn addition displayed clear grain boundaries without any

porosity or cracks. There were patches of black precipitates which might be Mn precipitates present in the grain boundaries, not being absorbed in the alloy matrix.

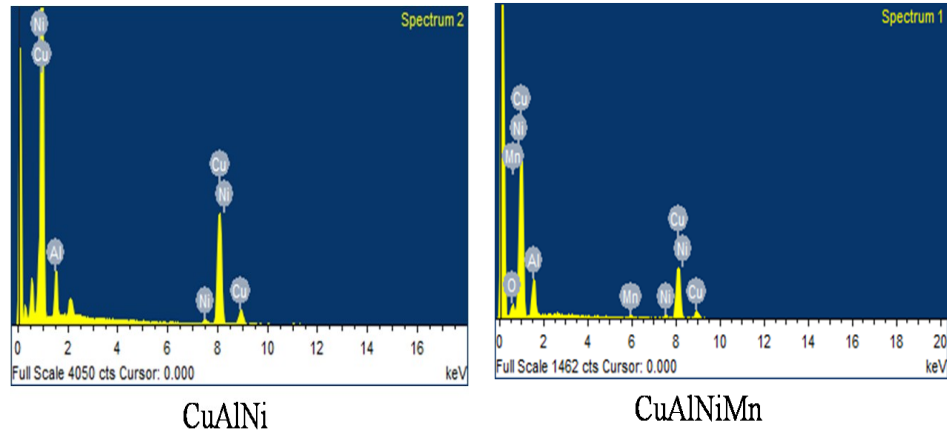


Figure 18 EDS compositional results for CuAlNi and CuAlNiMn SMA.

Table 2 Composition of each element in terms of weight.

Element	Weight% (CuAlNi Sample)	Weight% (CuAlNiMn Sample)
<b>O K</b>	6.98	9.74
<b>Al K</b>	14.13	13.02
<b>Ni K</b>	3.32	2.49
<b>Cu K</b>	75.57	70.62
<b>Totals</b>	100.00	100.00

The EDS analysis was performed at five different locations and the composition results are summarized in table (2). The composition analysis presented minor reduction in copper, nickel as manganese is added. Further, the adhesion of the

samples was characterized by employing scotch tape tests. Scotch tape of particular weight was cut and stuck to the bi-morph without and air gaps. Uniform pressure is applied and the sample is left for few minutes. The scotch tape is removed gradually and it is weighed again. There was less than 0.2 mg of sample adhering to the tape, demonstrating the excellent adhesion.

#### 4.1.2 Structural analysis

The XRD diffractogram showed the origin of crystalline  $\beta'_1$  martensite peak belonging to monoclinic structure. The sample developed with Mn addition showed  $\beta'_1$  (128) peak and the samples developed without Mn addition showed  $\beta'_1$ (208) peak. Fig. 19 shows the x-ray diffraction results of the bi-morphs. It is found that the pattern peaks were shifted towards a higher angle with variation in their shape and intensity, which were caused by the Mn addition.

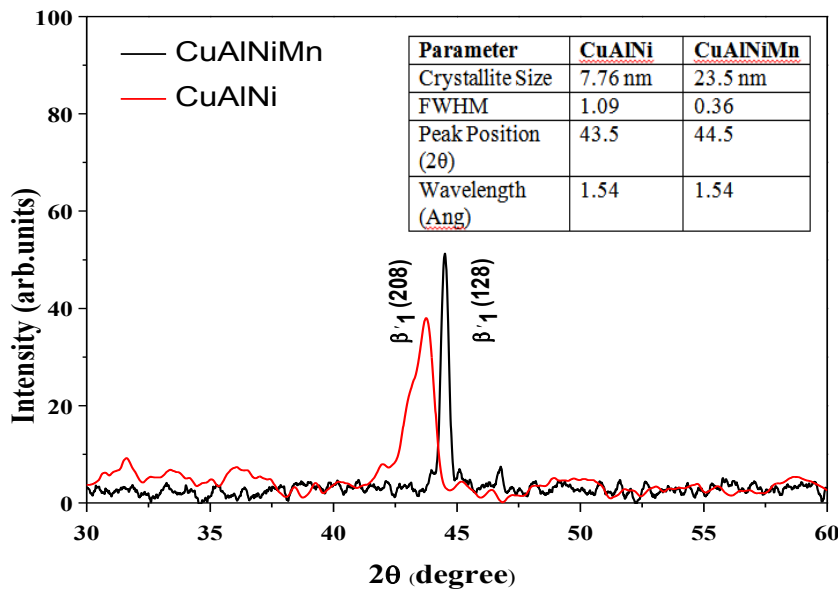


Figure 19 XRD analysis showing the origination of martensite peaks in the bi-morphs.

Similar reports regarding the peak shift has been reported by other reports [50,51]. The peaks were curve fitted using Gaussian fit and the FWHM values were obtained. The crystallite size calculated using the Scherrer formula was found to be 23.5 nm for the samples developed with Mn addition and CuAlNi/polyimide samples had crystallite size of 7.76 nm.

### 4.1.3 Thermal analysis

The differential scanning calorimetry analysis displayed the phase transformation temperature of the samples. The results show that Mn added samples had a reduced transformation temperature as compared to samples developed without Mn. The austenite transformation temperature  $A_s$  and  $A_f$  was found to be  $A_s - 220$  °C and  $A_f - 226$  °C respectively. As for the samples developed with Mn,  $A_s$  was 190 °C and  $A_f$  was 203 °C. There was no evidence of martensite transformation during cooling for both the samples. There were other peaks present in the samples which might be due to the stresses incurred during the deposition process[50,52]. Further these peaks might also be present because of other impurities, trapped gases or the glass transition of the polyimide substrate. Figure 7 shows the results of CuAlNi/polyimide and CuAlNiMn/polyimide samples. The TA of samples developed without Mn was 223 °C and for samples developed with Mn was 200 °C, as indicated by the green line in Fig. (20).

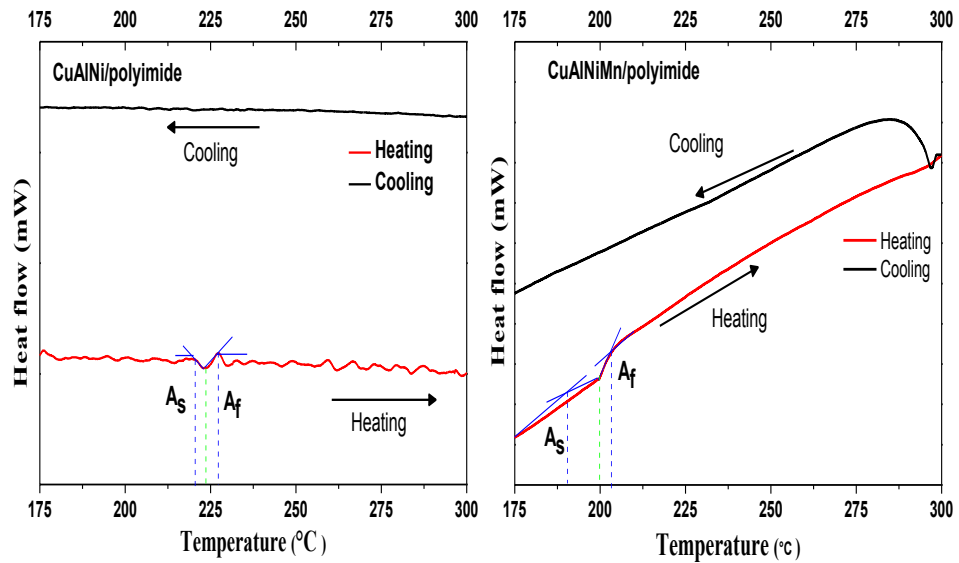


Figure 20: Differential Scanning calorimetry analysis showing the transformation temperatures.

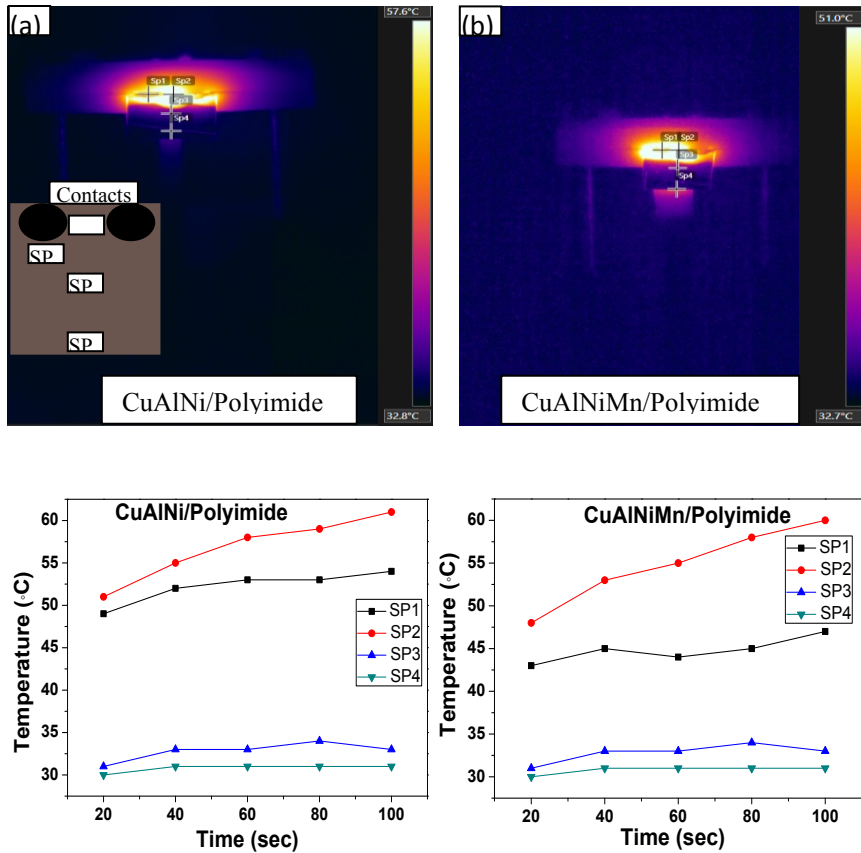


Figure 21 Thermal imaging of CuAlNi/Polyimide and CuAlNiMn/Polyimide bimorphs and its result.

Thermal images of the bi-morph were recorded using FLIR thermal camera and the temperature distribution of the film during actuation is presented in Fig. The temperature has been plotted at four different locations in the film. SP1 indicates the set point placed near the contacts, SP2 is placed in-between the contacts, SP3 is placed at the center of the film and SP4 is placed at the edge of the film. The temperature profile shows the SP2 temperatures is higher than the rest. SP1 temperature readings are slightly lower than SP2. SP3, and SP4 displayed less than 20 degrees difference from room temperature. Further the SP2 temperature profile of samples developed with Mn was lower than samples developed without Mn. Similar trend was observed with in the case of set point 1 with Mn added samples. The samples emissivity plays a vital role in indicating the temperature. The emissivity values were changes from 0.1 to 0.9 and the temperature values are recorded.

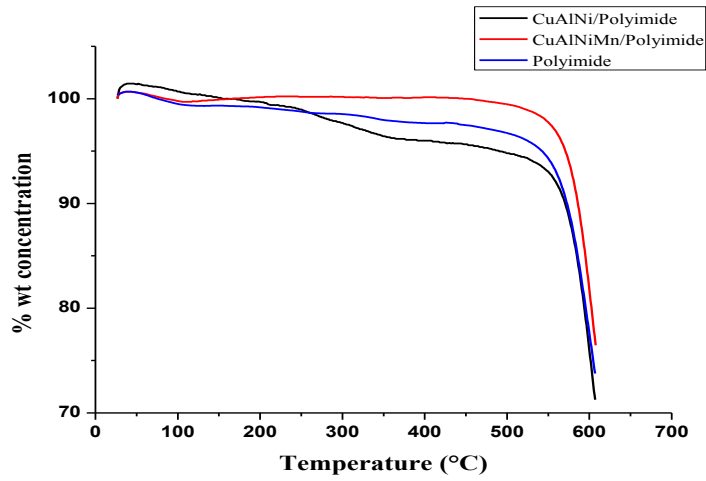


Figure 22 Thermogravimetric analysis for bare polyimide, CuAlNi/PI and CuAlNiMn/PI bimorphs.

Thermo-gravimetric results shows the rapid decomposition of CuAlNi/PI bimorph even at low temperature and it is even more as compare to bare polyimide.

Whereas Mn added SMA shows great thermo-stability even at high temperatures. There is no loss in weight of bimorph on addition of Mn. It starts decomposing only after 500<sup>0</sup>C and that too is because of melting of polyimide.

## 4.2 Tensile test

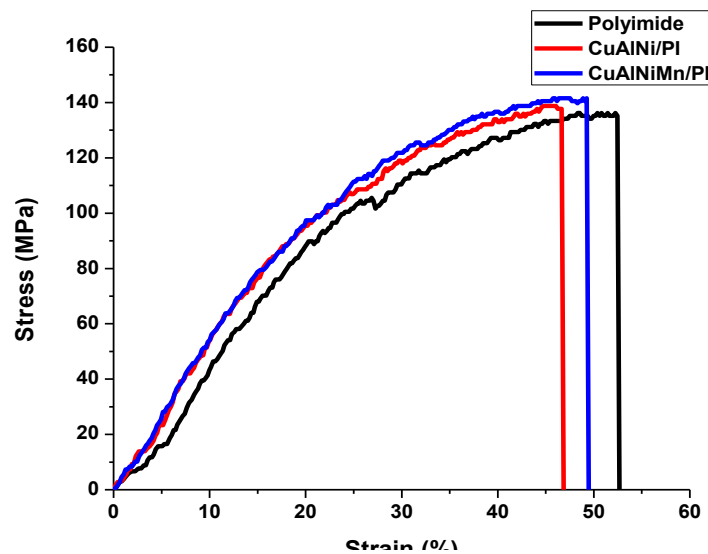


Figure 23 Comparison between stress-strain curve of polyimide and SMA bimorphs

#### 4.2.1 Comparison between Bimorphs and bare polyimide tensile test results:

Tensile test conducted on samples of size 50mm ×5mm and results are shown in the figure. From results it is confirmed that tensile strength of bimorphs has been increased compare to bare polyimide as SMA strength is added to it. Tensile strengths of polyimide, CuAlNi/PI and CuAlNiMn/PI are found to be 135.2 MPa, 137.72 MPa and 141.52 MPa respectively. But elongation to failure of bimorphs has been decreased because bimorph is under high tensile load at a particular elongation compare to bare polyimide because of added strength of SMA over it. Therefore, as soon as SMA over polyimide stops resisting the tensile load due to its complete breakage at a certain point and at this point high tensile stress due to combine effect of polyimide and SMA is greater than the tensile strength of polyimide which suddenly causes the failure before elongation limit of polyimide.

#### 4.2.2 Comparison between CuAlNi/PI and CuAlNiMn/PI bimorphs tensile test results:

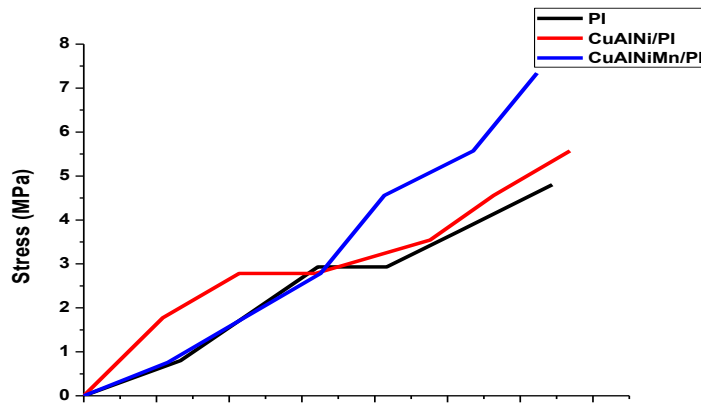


Figure 24 Closer view of stress-strain curve upto early 1.4% strain

It is observed that tensile strength as well as elongation to failure of CuAlNiMn/PI bimorph is increased compare to CuAlNi/PI bimorph. Tensile strength and elongation to failure of Mn added sample increased by 3.8 MPa and 2.6 mm respectively. But if observed the graph closely upto strain value of 1.4%, It can be easily seen that upto 0.4% strain CuAlNi/PI sample shows greater strength than Mn added sample but at a strain of 0.4% it starts to reduce and finally after 0.6% it shows lesser strength than Mn added sample. This behavior shows the brittle nature of CuAlNi film as brittle materials show very high yield

strength but fails suddenly without much elongation. This shows that CuAlNi film does not resist the tensile load for longer elongation of bimorph and eventually stops resisting the tensile load earlier than Mn added film which leads to early failure of CuAlNi/PI bimorph at less tensile stress with less elongation to failure compare to Mn added sample.

From tensile test results, it is observed that for the loads lesser than 1N, load bearing capacity of Mn added sample is very less compare to CuAlNi sample. This is may be the reason for more percentages reduction in displacement with increase in the loads and not lifting the higher loads on actuation for Mn added samples compare to CuAlNi samples.

### **4.3 Thermomechanical Analysis**

The thermomechanical behavior of the developed bi-morphs was tested at different voltages such as 1 V, 1.5 V and 2 V and at varying frequencies of 0.5 Hz, 0.33 Hz and 0.25 Hz for each loading conditions and the resulting graphs are plotted below.

#### **4.3.1 Load 30 mg**

Figure 9 (maximum displacement of 2.5 mm, 3.2 mm and 3.5 mm was observed from samples developed without Mn for three different frequencies. Whereas, CuAlNiMn samples showed 6.1 mm, 5.7 mm and 6.05mm was observed at frequencies of 0.5 Hz, 0.33 Hz and 0.25 Hz. Both the bi-morphs displayed steady actuation behavior at 0.25 Hz and 0.33 Hz and there was no deviation in displacement. With 1.5 V and 2 V at 0.5 Hz a), 9(c), and 9(e) shows the results obtained with CuAlNi/Polyimide bi-morphs and figure 9(b), 9(d), and 9(f) displays the results with CuAlNiMn/polyimide bi-morphs, under varying voltages and frequency for 20 seconds at 30 mg load. It is evident from the results that CuAlNiMn/Polyimide bi-morph has higher displacement than samples developed without Mn. At 2 V and 0.25 Hz as shown in figure 9(e) and

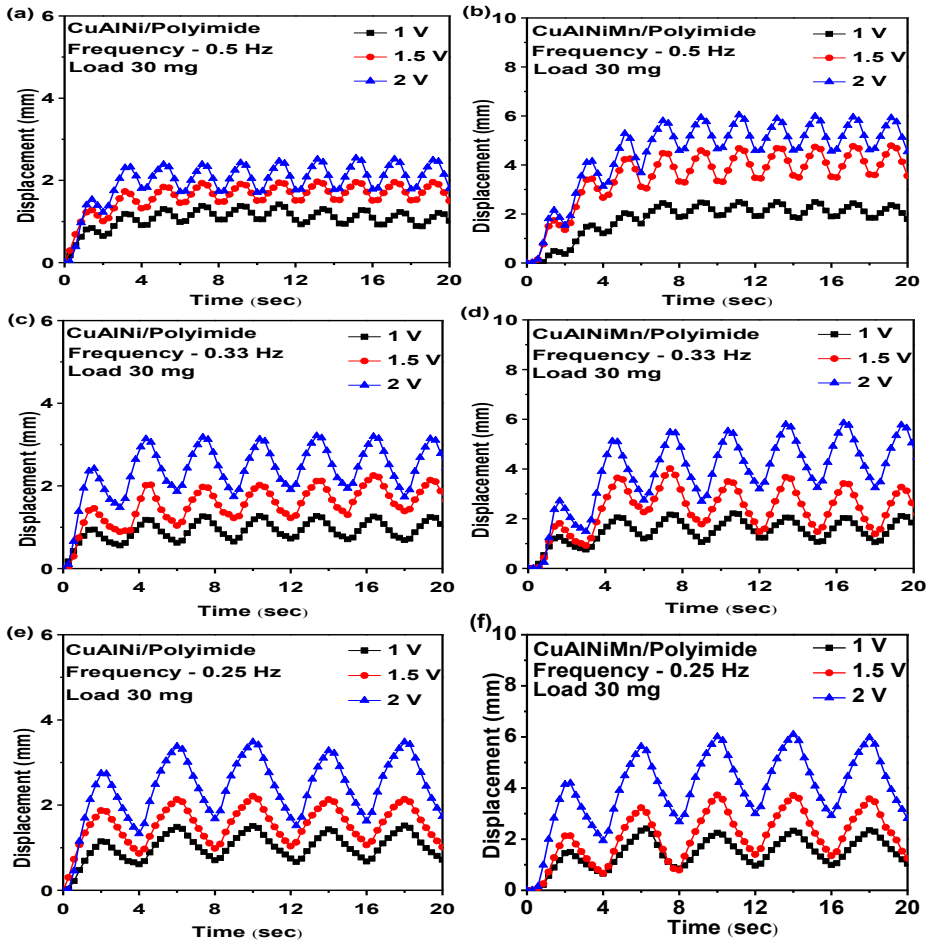


Figure 25 Electrical actuation results with 30 mg load at different voltages of 1 V, 1.5 V and 2 V (a) CuAlNi/Polyimide at 0.5 Hz (b) CuAlNiMn/polyimide at 0.5 Hz (c) CuAlNi/Polyimide at 0.33 Hz (d) CuAlNiMn/polyimide at 0.33 Hz (e) CuAlNi/Polyimide at 0.25 Hz

9(f), the displacement of Mn added samples were approximately 3.7 mm for one cycle, whereas samples developed without Mn exhibited maximum of 2.07 mm displacement. The displacement of both the samples reduced as the frequency was increased. On first heating cycle with 1 V and 0.5 Hz, both the bi-morphs displayed similar displacement readings however the displacement varied on subsequent cycles, as the film would have been at higher temperature than room temperature due to slow cooling through air convection. After few cycles, the displacement of the samples was consistent and a CuAlNi/Polyimide bi-morphs displayed minor fluctuation which was not observed with Mn added samples.

However, the fluctuations were not distinct in large no of cycles. Mn added samples exhibited higher displacement and steady actuation behavior with 30 mg load.

#### ***4.3.2 Load 45 mg***

As the load was increased to 45 mg, CuAlNi/Polyimide samples displayed a steady actuation behavior without any fluctuations. At voltages of 2 V the recorded displacement values for one cycle was 0.67 mm, 1.22 mm and 1.44 mm at varying frequency. There was no drastic variation with change in frequency as observed from figure 10(a), 10(c) and 10(e). The samples developed with Mn addition displayed improved displacement as compared to samples developed without Mn and displacement of 1 mm, 2.17 mm and 2.82 mm was observed at 2 V and three frequencies for one cycle as shown in figure 9(b), 9(d) and 9(f). However with higher frequency of 0.5 Hz the bi-morphs developed with Mn addition had difficulty in lifting the load and the on/off control was not sufficient to have precise control. For one cycle at 1 V and 0.5 Hz the displacement was 0.58 mm for samples with Mn and 0.32 mm for samples without Mn addition. The displacement was fluctuating; nevertheless there was no evidence of failure. Even though the ability to lift weights of 45 mg was not significant as compared to samples developed with Mn addition, Cu-Al-Ni/Polyimide samples exhibited steady and stable behavior.

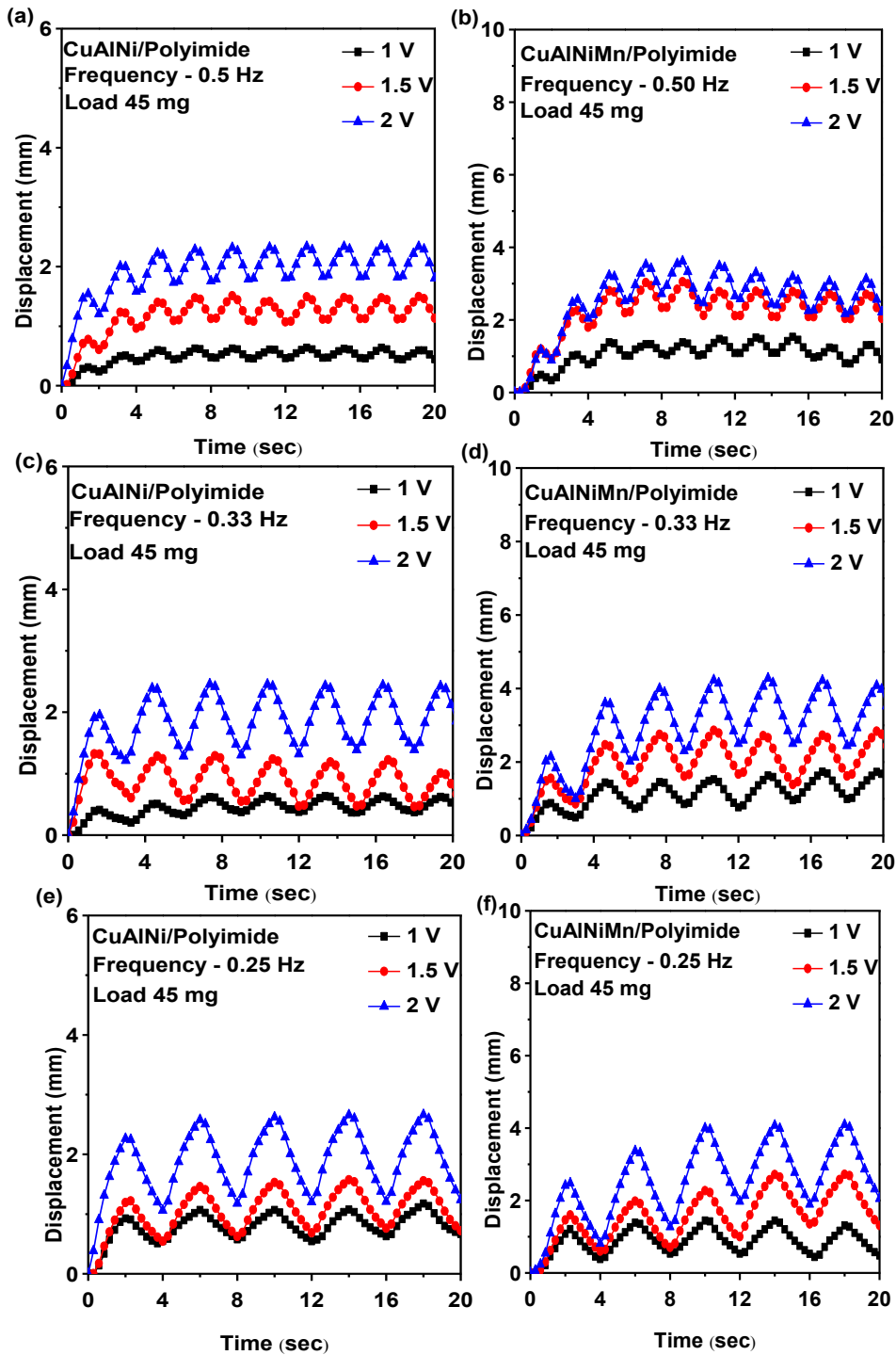


Figure 26 Electrical actuation results with 30 mg load at different voltages of 1 V, 1.5 V and 2 V (a) CuAlNi/Polyimide at 0.5 Hz (b) CuAlNiMn/polyimide at 0.5 Hz (c) CuAlNi/Polyimide at 0.33 Hz (d) CuAlNiMn/polyimide at 0.33 Hz (e) CuAlNi/Polyimide

### 4.3.3 Load 60 mg

The samples developed with Mn addition displayed a major difficulty in actuating under 60 mg loads. Figure 11(b), 11(d) and 11(f) shows the results of CuAlNiMn/ Polyimide bi-morph at varying actuation conditions. This behavior was evident at all the three frequencies with 1 V.

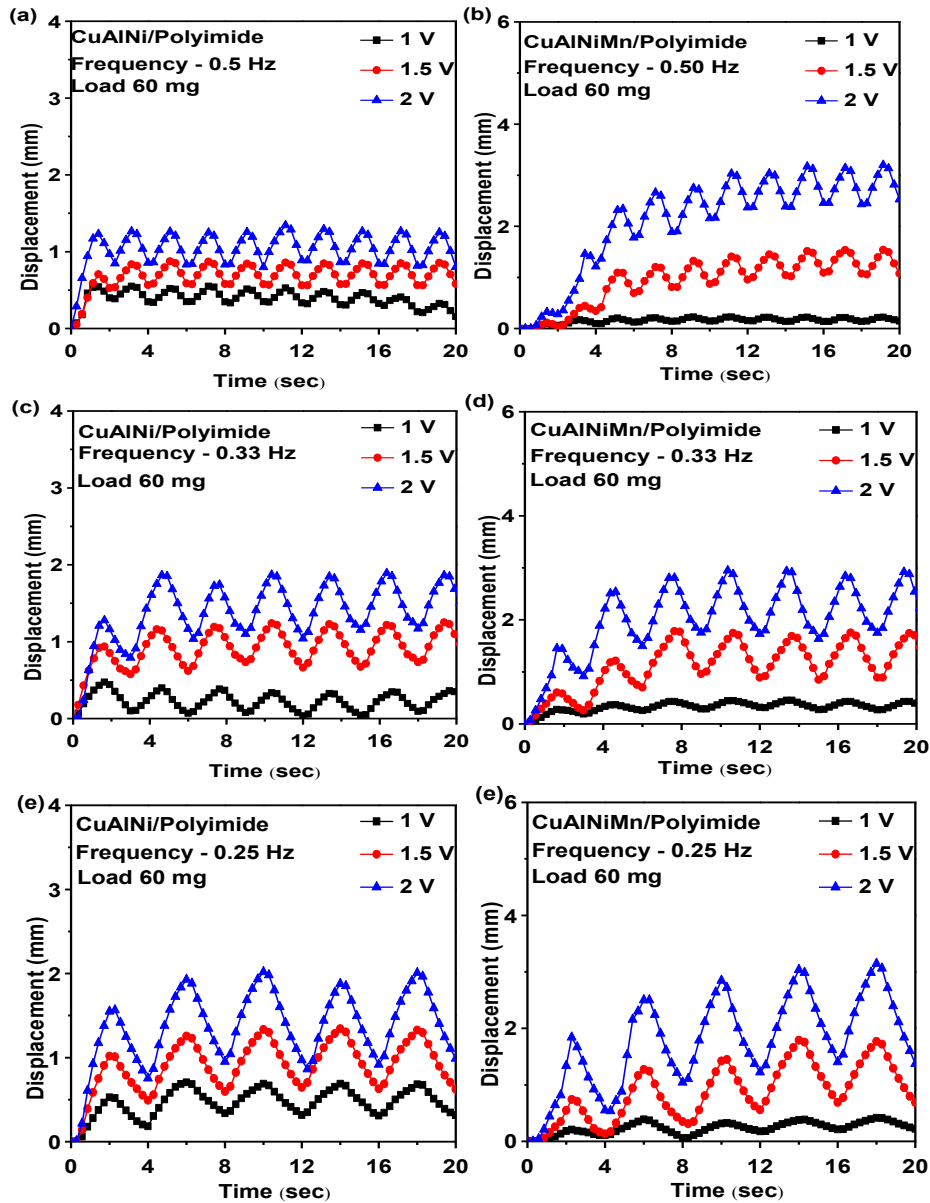


Figure 27 Electrical actuation results with 60 mg load at different voltages of 1 V, 1.5 V and 2 V (a) CuAlNi/Polyimide at 0.5 Hz (b) CuAlNiMn/polyimide at 0.5 Hz (c) CuAlNi/Polyimide at 0.33 Hz (d) CuAlNiMn/polyimide at 0.33 Hz (e) CuAlNi/Polyimide at 0.25 Hz

As the voltage was increased to 2 V, there was sufficient shape memory effect to lift the load and further the results displayed steady actuation behavior. The displacement under 60 mg loads was found to be approximately 0.08 mm, 0.28 mm and 0.35 mm at 2 V for one cycle. The effect of frequency on the samples was major, as all the samples exhibited increased displacement under varying actuation voltages. The samples developed without Mn addition, exhibited steady actuation properties at all conditions. Even at lower voltages of 1 V the thermomechanical behavior was definite with well-defined heating and cooling cycles. The average displacement at three different frequencies with 2 V was noticed to be 0.4 mm, 0.45 mm, and 0.52 mm for samples developed without Mn. The effect of frequency was minor at loads of 30 mg and 45 mg as observed from the thermomechanical analysis. Further from the analysis, the improvement of actuation was evident. However, the ability to actuate under higher loads was poor for samples developed with Mn. The primary reason might be the loss in toughness as the ductility increases.

#### ***4.3.4 Maximum Displacement***

Further to the actuation studies at different frequencies, the bi-morphs was tested with large heating and cooling cycle of 16 seconds, to find the maximum displacement under different loading conditions. Figures 12(a) to 12(i) shows the maximum displacements comparison plots under different actuation conditions. The plots reveal the enhanced displacement exhibited by Mn added samples. Further, it can be clearly seen that CuAlNiMn film takes more than 0.5 seconds to actuate, indicating the time required to reach austenite phase. Whereas, CuAlNi film actuates immediately, exhibiting better sensitivity to transform faster with Joule heating. Figures 12(a) and 12(d) are some of the plots displaying the better sensitivity behavior of CuAlNi/Polyimide bi-morphs. Even though CuAlNi has better sensitivity, the response time of Mn added samples were significantly better than samples developed without Mn addition.

It is seen that CuAlNi film does not exhibit considerable displacement after 5 second of heating and a flat curve on time vs displacement graph is observed.

Whereas, CuAlNiMn film shows rapid displacement till 5 seconds and as the rate of displacement slightly decreases the curve tends to be flat after 7.5 seconds of heating. Mn added samples exhibited faster heating and cooling rate as compared to samples developed without Mn and thereby actuating for extended periods. The cooling curve showed the bi-morphs returned to its original position in most of the actuation conditions with a very minor loss in displacement. It can be observed from the graphs that load carrying capacity of CuAlNiMn film is less as load increases to 60 mg. The maximum displacement graphs with loads of 30 and 45 mg, CuAlNiMn film shows displacement which is almost twice the displacement of CuAlNi film for all the three voltages.

However, as load increases to 60 mg, the difference between displacement of CuAlNiMn and CuAlNi films reduces considerably as compared to 30 mg and 45 mg loads for all the three voltages. At 1 V and 60 mg load at the free end of bi-morph, CuAlNiMn film shows very less displacement than CuAlNi film. Thus at lower voltages force generated by CuAlNiMn film on phase transformation is not sufficient to carry higher loads. This can be seen from the maximum displacement graphs at a particular voltage of 1 V for actuation. On the other hand CuAlNi produces sufficient force to move the 60 mg load even at low voltage of 1V. It is observed that there is no considerable change in the maximum displacement of CuAlNi film with three different loads and at a particular voltage value. Maximum displacement of 5.7 mm was observed with Mn added samples and 2.8 mm was observed with samples developed without Mn at 2 V and 30 mg load.

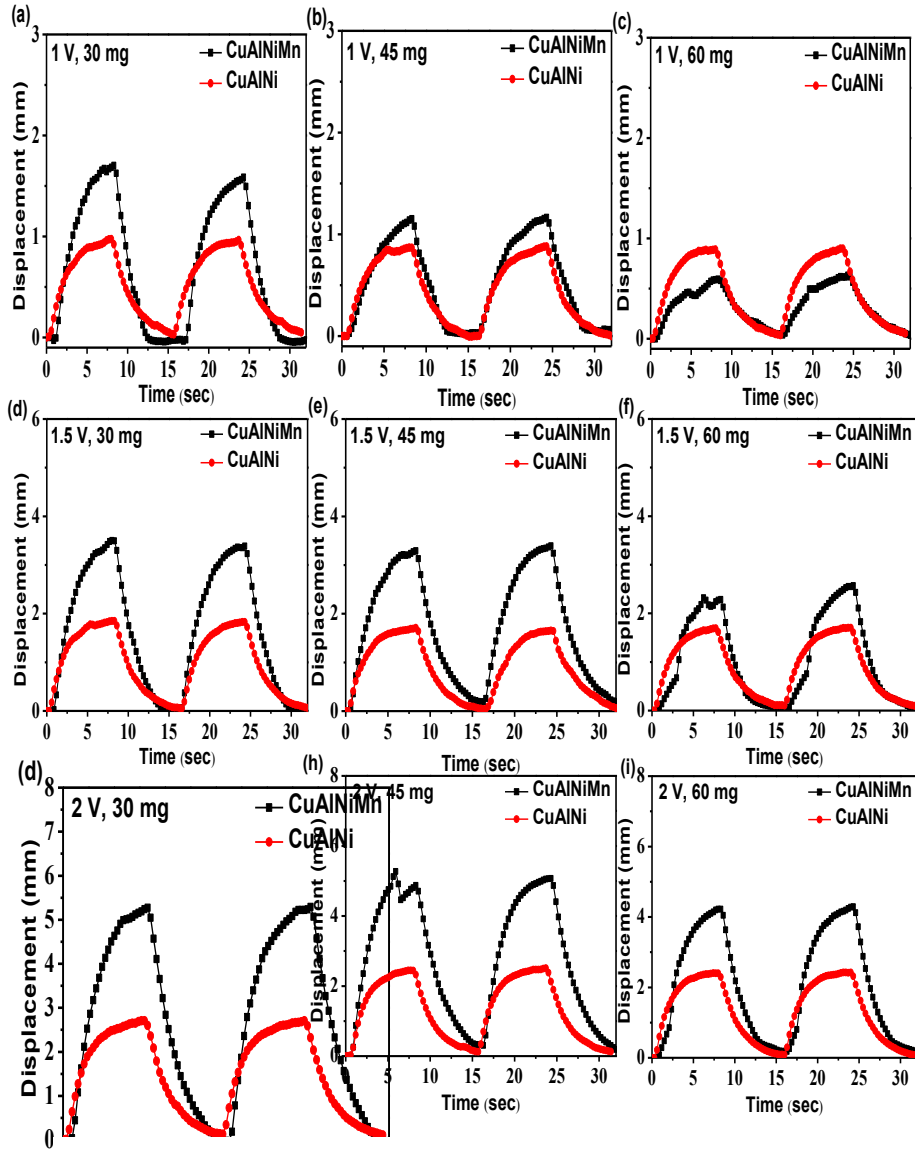


Figure 28 Electrical actuation results comparing the maximum displacement of CuAlNi/polyimide and CuAlNiMn/polyimide samples at varying load and varying voltages. (a) 1 V, 30 mg (b) 1 V, 45 mg (c) 1 V, 60 (d) 1.5 V, 30 mg (e) 1.5 V, 45 mg (f) 1.5 V, 60 mg

#### 4.3.5 Discussion

Grain boundary strengthening is one of the primary mechanics to increase the strength of the material in poly crystalline material. Decreasing or increasing the grain size is effective only to certain extent. The relation between the grain size and the strength of the material is given by Hall-Petch equation and it states the maximum attainable yield strength is experimentally found to be with grains of 10

nm. Grains can be assumed to be arrangement of perfectly aligned atoms, according to the crystal structure of the material. Boundaries which separate the different orientations of the atoms are as grain boundaries. The movement of linear defects or dislocations in a crystal lattice. Deformation in any material can be visualized as movement of linear defects known as dislocations in an crystal lattice. For a particular crystal structure, dislocations move in an preferred direction in an preferred plane (generally the direction of highest atomic density in the plane of highest atomic density). This movement will be impeded by the change in orientation of crystals. With higher stress, the dislocation pile up begins to grow as more and more dislocations get stuck at the same grain boundary. Also as stress begins to increase, larger amount of dislocation are generated within the material. When applied stress exceeds critical breaking stress of grain boundary, the dislocations begin to flow through grain boundaries.

Now, smaller the grain size, higher is the grain boundary area per unit volume. So there is a higher probability of an dislocation getting stuck at a grain boundaries. Consequently, a higher concentration on dislocations can be accommodated in a unit volume of material with lower grain size without allowing material to flow. This leads to requirement of higher number of dislocations to begin flow of the material, termed as "yielding" of material commonly. In this manner, smaller grains lead to higher strength.

The shape memory effect in CuAlNi is exhibited at specific composition of 11-14 wt.% for aluminum and 3-5 wt.% for nickel. Additionally, to control/ slow down the diffusivity of Cu and Al, nickel was added. CuAlNi shape memory alloys are susceptible to intergranular fracture and thereby leading to fracture within stress level of 300 Mpa. It also affects the mechanical properties of the film. Mn addition increase the ductility by

The microscopic images reveal the increase in grain size distinctly on the addition of Mn. Further the grain boundaries are more compared to the samples developed without Mn, which in turn affects the electrical conductivity of the film. This might be one of the reasons for the improved displacement as observed with Mn

added samples. Large grain have less boundaries and their electrical and mechanical properties such as resistance and toughness decreases. Further to support this, the XRD peaks also displayed a larger crystallite size as compared to samples developed without Mn addition. The diffractogram also revealed the crystalline monoclinic peak without any  $\alpha$  or  $\gamma$  phases. This shows the ability of the Mn added samples to have better cyclic repeatability. The composition analysis exhibited an increase in Al content which might be due to the diffusion of Mn in the alloy as witnessed from the SEM analysis. The load bearing capacity of Mn added samples was affected due to the increase in grain size as observed from the results obtained with 60 mg loads. As the grain size increases the ductility improves and the toughness of the samples decreases. This was distinct with the experiments to find the maximum displacement. Mn added samples failed to bear higher loads and their actuation was not significant as compare to CuAlNi/polyimide samples. This was further evident from the tensile test results, which displayed lower yield strength for samples developed with Mn. This shows the ductile nature of CuAlNiMn SMA as it requires less force for elongation compare to the force required for elongation of CuAlNi SMA with the same amount. The thermal analysis exposed a lower transformation temperature which may possible be the reason for their superior rate of actuation during heating and cooling cycles. The thermal analysis showed a difference of 20 °C between the two samples which might affect the sensitivity of samples, as witnessed from the frequency actuation. The bare polyimides thermal history will also affect the sensitivity drastically[53]. The large duration of actuation for CuAlNiMn film is predominantly due to their wide range of austenite transformation temperature and high conductivity. The conductivity of the film plays a vital role during electrical heating as there is more flow of current at higher voltages. When the voltage is less, flow of current in the film is minimum and therefore slower response[54]. Heat generated in the film is proportional to the square of current, hence small increase in current drastically increases the temperature of the film and we achieve more shape recovery at high temperature. The frequency actuation results displayed the behavior of CuAlNi/polyimide and CuAlNiMn/polyimide bi-

morphs thermomechanical behavior at various actuation conditions. From the results the effect of Mn addition has enhanced the thermomechanical response of copper based shape memory alloys. This shows that there is improvement in the ductility but reduction in the toughness of CuAlNi SMA on addition of Mn. The displacement of the samples at 1.5 V and 2 V particularly exhibited increased displacement with two orders higher than samples developed without Mn.

# Chapter 5 Life cycle behavior of CuAlNi/PI and CuAlNiMn/PI bimorph

## 5.1 Life cycle of CuAlNi/PI bimorph

Life cycle behavior of CuAlNi/PI bimorph was studied by performing actuation experiments with eight different samples of same size and shape as is used in the study of thermomechanical behaviour of CuAlNi/PI bimorph. Figure(30) shows the results for life cycle behaviour of CuAlNi/PI and bimorph. Actuation experiment was performed at actuation voltage of 2V to avoid overheating and to avoid early failure of CuAlNi SMA thin film due to burning and also is to avoid multiple failure mode of bimorph. Out of three frequencies which were used for thermomechanical behavior, higher frequency actuation was preferred for the experiments. Load of 45 mg was chosen for life cycle experiment as it is lifted by both the bimorphs easily. Plan was to go for maximum load i.e. 60 mg but as Mn added samples are having difficulty in carrying 60 mg load which harms the cyclic repeatability of Mn added bimorph, load of 45 mg was chosen for the experiments. Failure was defined to be 50% loss in actuation and each sample was allowed to actuate upto 15000 cycles as first few failures occurred under it, so number of cycles were also fixed.

Out of eight samples, two samples could run beyond 15000 cycles and experiment for that particular sample was stopped after it. One sample showed early life failure and could run only for 5452 cycles. This is the earliest failure among all the samples. In general, the loss of actuation property starts gradually over the no. of cycles. But with CuAlNi thin film, in addition to that one more failure mode was observed and i.e. breakage of SMA thin film due fatigue. This is because of brittle nature of CuAlNi film which is very susceptible intergranular cracking in cyclic loading Table (3) shows all the failure related data.

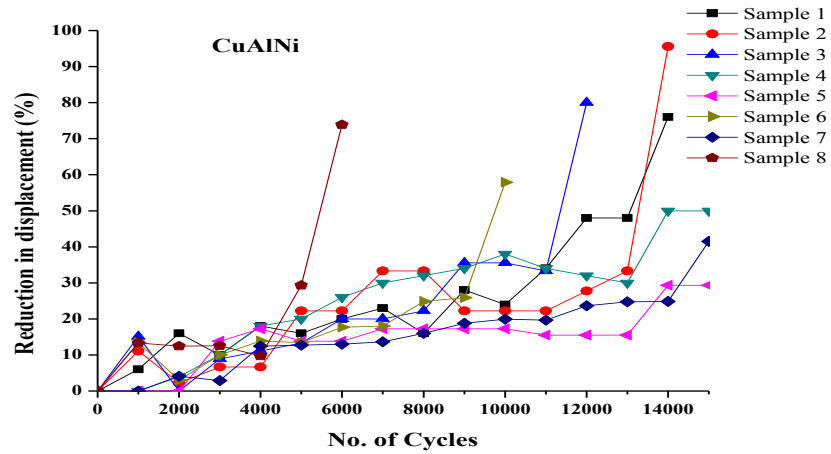


**Figure 29 Life cycle behavior of CuAlNi/PI bimorph**

**Table 3 Life cycle data for CuAlNi/PI bimorph**

Sample Code	State	Cycles to failure
1	F	13534
2	F	13283
3	F	11657
4	F	13967
5	S	15000
6	F	10768
7	S	15000
8	F	5862

It was observed from the results that there are sudden failure in most of the samples. These are due to the brittle nature of the CuAlNi SMA film. Number of micro cracks propagate and accumulates at a certain point near the fixed end of actuator which is responsible for fracture failure because maximum stresses

generates at fixed point of cantilever due to deflection. Fig (31) shows the digital microscopic images of a CuAlNi/PI sample before and after failure.

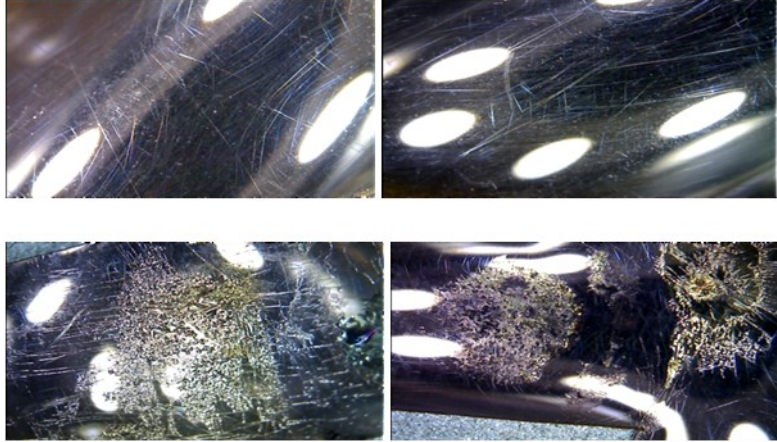


**Figure 30 Digital microscopic image of deposited sample before actuation, Digital microscopic image of failed component after actuation.**

## **5.2 Life cycle of CuAlNiMn/PI bimorph**

Life cycle experiments were also performed for CuAlNiMn/PI bimorph with the same parameters such as voltage, frequency of actuation and load, defined failure which were used for CuAlNi/PI bimorph. Here in case of CuAlNiMn/PI bimorph very first sample out of eight tested samples was survived for more than 25000 cycles. After that, four samples were failed in the range of 14000 to 19000. Therefore maximum no. of cycles which were to be performed on the samples were fixed to 25000 cycles. Three samples out of eight tested samples were survived for 25000 cycles. Figure(32) shows the life cycle behavior of eight Mn added samples. Further digital microscopic images were taken for failed samples Figure() a & b and it was found from the images that there is a sign of CuAlNiMn thin film peel off near fixed end of cantilever for the sample which could run for 25000 cycles and complete peel off at fixed end for the sample which got failed

under 25000 cycles. CuAlNiMn/PI bimorph got better actuation as well as longer life compare to CuAlNi/PI bimorph.

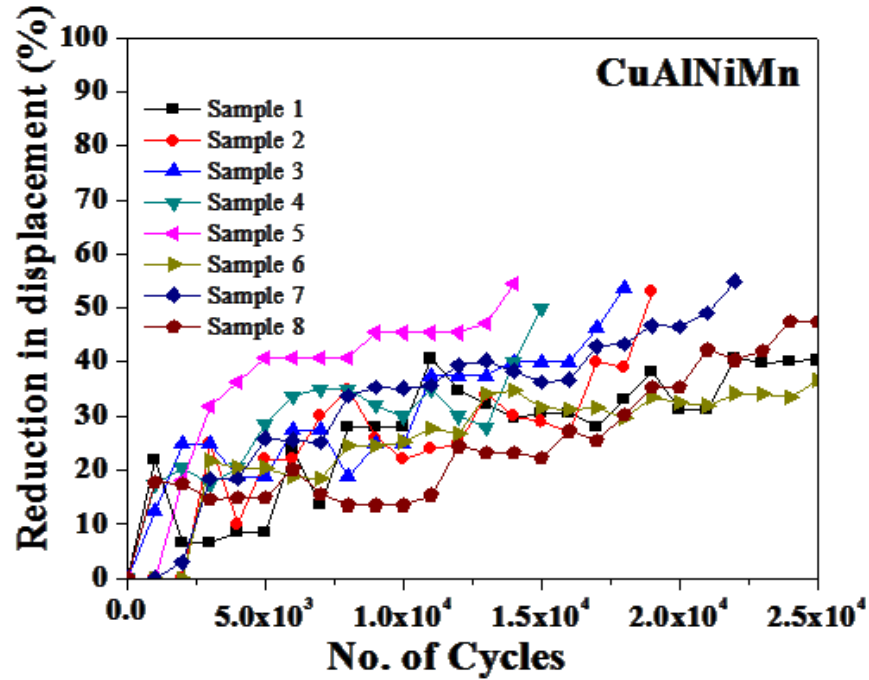


Figure 31 Life cycle of CuAlNiMn bimorph

Table 4 Life cycle data for CuAlNi/PI bimorph

Sample Code	State	Cycles to failure
1	S	25000
2	F	18678
3	F	17892
4	F	15675
5	F	13597
6	S	25000
7	F	21263
8	S	25000

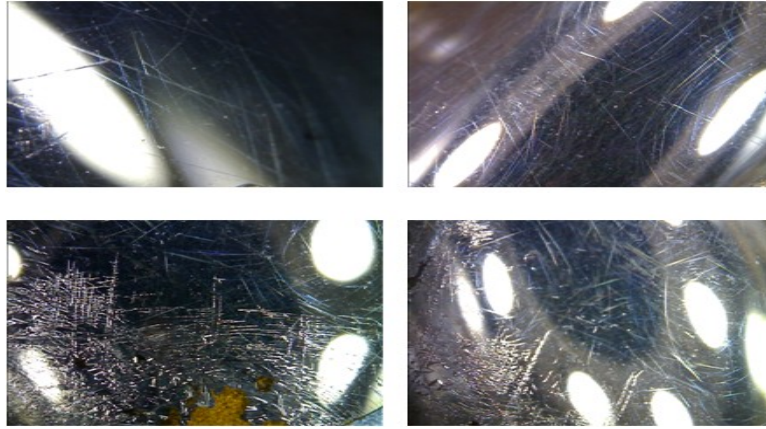


Figure 32 Digital microscopic image of deposited sample before actuation, Digital microscopic image of failed component after actuation.

Here, in case of CuAlNiMn/Polyimide, there is no abrupt failure of film but it gradually loss its actuation which was not the case with CuAlNi/Polyimide bimorph.

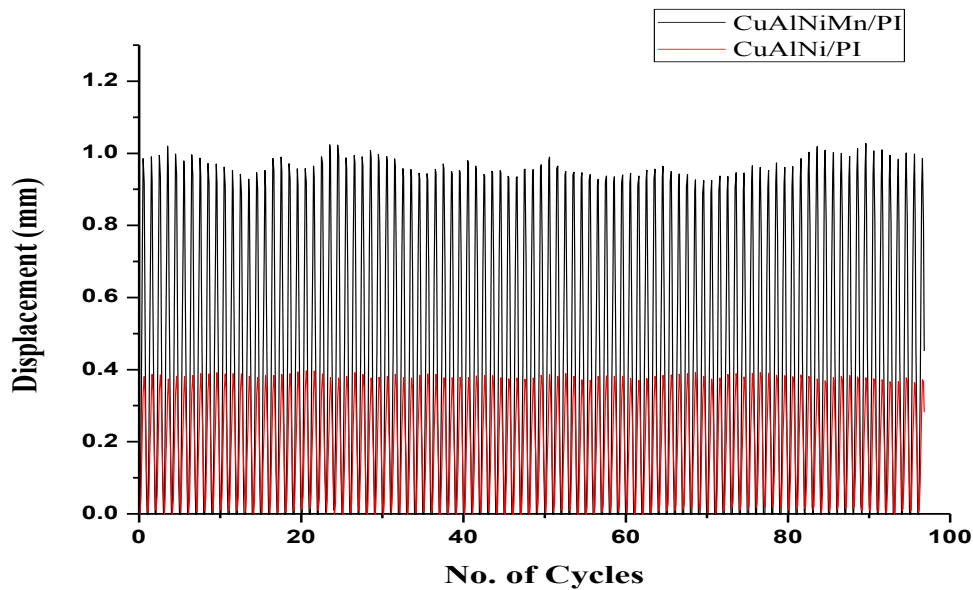


Figure 33 Repeatability in Life cycle behaviour experimental result

Figure(34) shows the smaller part of about 100 cycles from the life cycle behavior results which shows preciseness in position of both Mn added and

without Mn added bimorph samples. Excellent repeatability of cyclic behaviour has been achieved with both the bimorphs.

### 5.3 Reliability results:

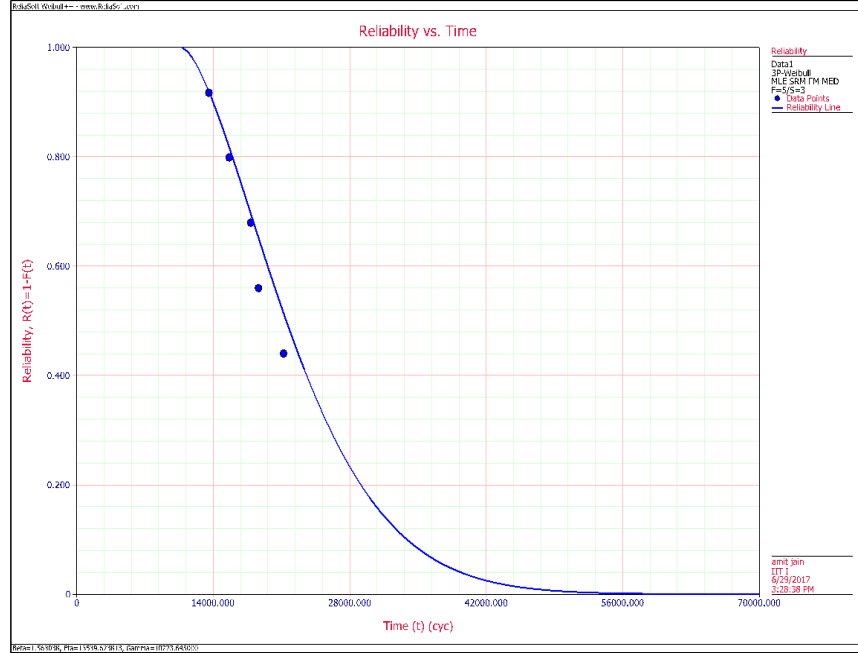


Figure 34 Reliability vs Time relationship for CuAlNiMn/PI bimorph

Reliability vs Time relationship was found from Reliasoft software using Weibull++ tool. Life data for CuAlNiMn/PI bimorph has got three parameter Weibull distribution as a best distribution for it. Third parameter is  $\gamma$  which is called as location parameter which tells that upto that time, there will not be any failure.

Reliability function for 3P Weibull distribution is given as,

$$R(t) = e^{-\left(\frac{t-\gamma}{\eta}\right)^\beta}$$

$$\beta = 1.56, \eta = 13539.62, \gamma = 10773.65$$

Similarly, for the life data of CuAlNi/PI bimorph two parameter Weibull distribution was found to be the best. Reliability function for two parameter Weibull distribution is given as,

$$R(t) = e^{-\left(\frac{t}{\eta}\right)^\beta}$$

$$\beta = 4.47, \eta = 14068.68$$

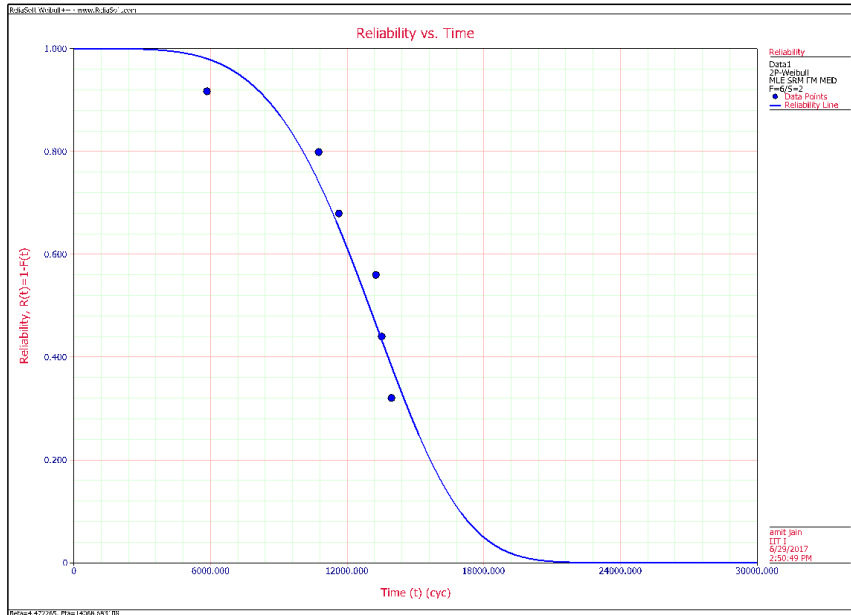


**Figure 35 Reliability vs Time relationship for CuAlNi/PI bimorph**

It is observed from the plots that reliability of CuAlNiMn/PI bimorph has been improved drastically than CuAlNi/PI bimorph.

# Chapter 6 Conclusion and future scope

## Conclusion

The thermomechanical behavior of CuAlNiMn/polyimide bi-morphs has been investigated in detail under varying actuation conditions. It can be concluded that Mn addition definitely improves the thermomechanical response of the shape memory alloy. The addition of Mn to CuAlNi shape memory alloy improves its electrical conductivity and increases its ductility. However it fails to actuate under higher loads. The results can be summarized as

- Mn added samples displayed higher displacement and higher rate of heating due to their improved grain size.
- The sensitivity was better for samples developed without Mn, as actuation was significant under higher loads.
- Load bearing capacity of Mn added samples is reduced due to lower yield strength.

## Future Scope

Both the developed bi-morphs exhibited a steady and stable actuation behavior without any failure. The detailed analysis could be utilized as platform to develop microactuators for different applications. Maximum displacement of 5.75 mm could be achieved by the addition of Mn to CuAlNi shape memory alloy at 2 V and 30 mg load. The frequency actuation and load bearing capacity analysis can be used as a parameter set to develop microflapper, microgrippers and microcantilevers. Further studies on the mechanical properties will lead to development of highly efficient actuators.

To broaden the applications of shape memory alloys the developed bi-morphs can be used as a microflapper in aerial robots, where the bi-morphs can be utilized as wings. The bi-morphs have been tested with high frequency of 20 Hz at

laboratory level. As the load bearing capacity of the bi-morphs has been tested. Improvements on design can be made to expand the shape memory properties. Further uses on utilizing the bi-morph in temperature sensing[55] and ballistic applications can be probed as these alloys have excellent actuation and damping properties.

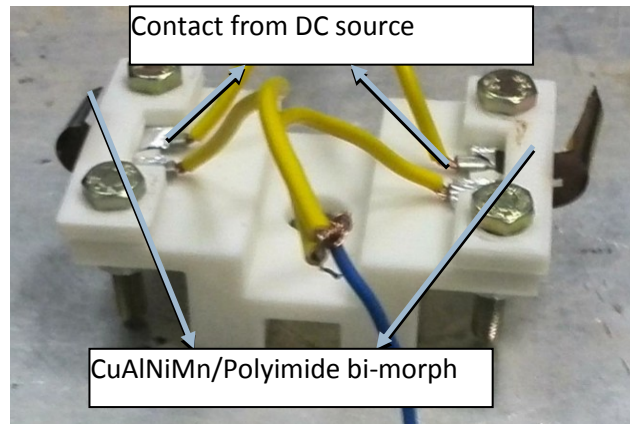


Figure 36 Proposed design of the aerial robot with SMA bi-morph

# Chapter 7 Bibliography

- [1] Dimitris C. Lagoudas, Shape Memory Alloys: Modeling and Engineering Applications, Springer, 2008. doi:10.1007/978-0-387-47685-8.
- [2] K.L. Sundarkrishnaa, Springer Series in Materials Science, 2012. doi:10.1007/978-3-642-33848-9.
- [3] C. Menna, F. Auricchio, D. Asprone, Applications of Shape Memory Alloys in Structural Engineering, 2015. doi:10.1016/B978-0-08-099920-3.00013-9.
- [4] C.. K Otsuka, C.M Wayman, Shape Memory Materials, 1998.
- [5] T. Duerig, K. Melton, D. Stockel, C. Wayman, Engineering aspects of shape memory alloys, 1990. <http://scholar.google.com/scholar?hl=en&btnG=Search&q=intitle:Engineering+Aspects+of+Shape+Memory+Alloys#0>.
- [6] K.T. and S.M. K. Yamauchi, I. Ohkata, Shape memory and superelastic alloys Technologies and applications, 2011. [http://books.google.com/books?hl=en&lr=&id=xpSlAgAAQBAJ&oi=fnd&pg=PA355&dq=Shape+memory+and+superelastic+alloys&ots=0YUjykG\\_Pk&sig=Mt\\_pfhNatW4h2PJJ2A4\\_BchEvsU](http://books.google.com/books?hl=en&lr=&id=xpSlAgAAQBAJ&oi=fnd&pg=PA355&dq=Shape+memory+and+superelastic+alloys&ots=0YUjykG_Pk&sig=Mt_pfhNatW4h2PJJ2A4_BchEvsU).
- [7] W.M. Huang, Z. Ding, C.C. Wang, J. Wei, Y. Zhao, H. Purnawali, Shape memory materials, Mater. Today. 13 (2010) 54–61. doi:10.1016/S1369-7021(10)70128-0.
- [8] K. Otsuka, X. Ren, Recent developments in the research of shape memory alloys, 7 (1999) 511–528.
- [9] A. Leppäniemi, Shape memory alloys – applications and commercial aspects, (2000) 1–16. <http://www.ac.tut.fi/aci/courses/76527/Seminars2000/SMA.pdf>.
- [10] L. Sun, W.M. Huang, Z. Ding, Y. Zhao, C.C. Wang, H. Purnawali, C. Tang, Stimulus-responsive shape memory materials: A review, Mater. Des. 33 (2012) 577–640. doi:10.1016/j.matdes.2011.04.065.
- [11] C. LExcellent, Shape-memory Alloys Handbook, 2013. doi:10.1002/9781118577776.
- [12] S. Wei, Z. G.; Sandstroröm, R.; Miyazaki, Review Shape memory materials and hybrid composites for smart systems, J. Mater. Sci. 33 (1998) 3743–3762. doi:10.1023/A:1004692329247.
- [13] E. Engineers, Compliant Modular Shape Memory Alloy Actuators, (2014).

- [14] J.S. Juan, G.A. López, J. Chengge, M.L. Nó, D. Física, M. Condensada, P. Vasco, F. De Ciencia, Nano-scale Superelastic behavior of Shape Memory Alloys for potential MEMS applications, (2000) 2–3. doi:10.1016/j.jallcom.2011.10.110.
- [15] Y. Bellouard, Shape memory alloys for microsystems: A review from a material research perspective, *Mater. Sci. Eng. A.* 481–482 (2008) 582–589. doi:10.1016/j.msea.2007.02.166.
- [16] Y. Fu, H. Du, W. Huang, S. Zhang, M. Hu, TiNi-based thin films in MEMS applications: A review, *Sensors Actuators, A Phys.* 112 (2004) 395–408. doi:10.1016/j.sna.2004.02.019.
- [17] D. Hartl, D.C. Lagoudas, Aerospace applications of shape memory alloys, *Proc. Inst. Mech. Eng. Part G J. Aerosp. Eng.* 221 (2007) 535–552.
- [18] J. Mohd Jani, M. Leary, A. Subic, M. a. Gibson, A review of shape memory alloy research, applications and opportunities, *Mater. Des.* 56 (2014) 1078–1113. doi:10.1016/j.matdes.2013.11.084.
- [19] S. Miyazaki, Y.Q. Fu, W.M. Huang, Overview of sputter-deposited TiNi based thin films, 2009. doi:<https://doi.org/10.1557/mrs2002.43>.
- [20] O. Kastner, G.J. Ackland, Mesoscale kinetics produces martensitic microstructure, *J. Mech. Phys. Solids.* 57 (2009) 109–121. doi:10.1016/j.jmps.2008.09.016.
- [21] D. Roqueta, F.C. Lovey, M. Sade, The hysteresis in the martensitic transformations due to the interaction with precipitates in Cu-Zn-Al alloys, *Scr. Mater.* 34 (1996) 1747–1752. doi:10.1016/1359-6462(96)00050-4.
- [22] Y.F. Guo, Y.S. Wang, D.L. Zhao, W.P. Wu, Mechanisms of martensitic phase transformations in body-centered cubic structural metals and alloys: Molecular dynamics simulations, *Acta Mater.* 55 (2007) 6634–6641. doi:10.1016/j.actamat.2007.08.018.
- [23] S. Agouram, M.O. Bensalah, A. Ghazali, A MICROMECHANICAL MODELLING OF THE HYSTERETIC BEHAVIOUR IN THERMALLY INDUCED MARTENSITIC PHASE TRANSITIONS: APPLICATION TO  $\text{Cu} \pm \text{Zn} \pm \text{Al}$  SHAPE MEMORY ALLOYS, 47 (1999).
- [24] W. Huang, On the selection of shape memory alloys for actuators, *Mater. Des.* 23 (2002) 11–19.
- [25] V. Torra, a. Isalgue, F.C. Lovey, M. Sade, Shape memory alloys as an effective tool to damp oscillations, *J. Therm. Anal. Calorim.* 119 (2015) 1475–1533. doi:10.1007/s10973-015-4405-7.
- [26] S. Cabrera, N. Harrison, D. Lunking, R. Tang, Shape Memory Alloy Latching Microactuator, *Mse.Umd.Edu.* (2002).

[http://www.mse.umd.edu/undergrad/490\\_materials\\_design/490\\_fall\\_2002/490\\_fall2002\\_final\\_project\\_results/enma490\\_fall02\\_final\\_report\\_121202.pdf](http://www.mse.umd.edu/undergrad/490_materials_design/490_fall_2002/490_fall2002_final_project_results/enma490_fall02_final_report_121202.pdf).

- [27] S.K. Sadrnezhad, N. Yasavol, M. Ganjali, S. Sanjabi, Property change during nanosecond pulse laser annealing of amorphous NiTi thin film, *Bull. Mater. Sci.* 35 (2012) 357–364. doi:10.1007/s12034-012-0293-7.
- [28] Z.L.C. Zhang, J. X., Liu, Y. X., Cai, W., The mechanisms of two way-shape memory effect in a Cu-Zn-Al alloy, *Mater. Lett.* 33 (1997) 211–214.
- [29] E. Cingolani, M. Ahlers, M. Sade, The two way shape memory effect in Cu-Zn-Al single crystals: role of dislocations and stabilization, *Acta Metall. Mater.* 43 (1995) 2451–2461. doi:10.1016/0956-7151(94)00415-3.
- [30] E. Cingolani, M. Ahlers, On the origin of the two way shape memory effect in Cu-Zn-Al single crystals, *Mater. Sci. Eng. A.* 273–275 (1999) 595–599. doi:10.1016/S0921-5093(99)00436-0.
- [31] B. Chen, C. Liang, D. Fu, D. Ren, Corrosion behavior of Cu and the Cu-Zn-Al shape memory alloy in simulated uterine fluid., *Contraception.* 72 (2005) 221–4. doi:10.1016/j.contraception.2005.04.006.
- [32] N. Haberkorn, F.C. Lovey, a. M. Condó, J. Guimpel, Development and characterization of shape memory Cu-Zn-Al thin films, *Mater. Sci. Eng. B.* 170 (2010) 5–8. doi:10.1016/j.mseb.2010.01.058.
- [33] S. Longauer, P. Makroczy, G. Jana, M. Longauerova, Shape memory effect in a Cu – Zn – Al alloy with dual phase a / b microstructure, 275 (1999) 415–419.
- [34] M. Guerioune, Y. Amieur, W. Bounour, O. Guellati, a. Benaldjia, a. Amara, N.E. Chakri, M. Ali-Rachedi, D. Vrel, SHS of shape memory CuZnAl alloys, *Int. J. Self-Propagating High-Temperature Synth.* 17 (2008) 41–48. doi:10.3103/S1061386208010044.
- [35] V. Recarte, I. Hurtado, J. Herreros, M.L. Nó, J. San Juan, Precipitation of the stable phases in Cu-Al-Ni shape memory alloys, *Scr. Mater.* 34 (1996) 255–260. doi:10.1016/1359-6462(95)00493-9.
- [36] F.M. Braz Fernandes, K.K. Mahesh, R.M.S. Martins, R.J.C. Silva, C. Baehtz, J. von Borany, Simultaneous probing of phase transformations in Ni-Ti thin film shape memory alloy by synchrotron radiation-based X-ray diffraction and electrical resistivity, *Mater. Charact.* 76 (2013) 35–38. doi:10.1016/j.matchar.2012.11.009.
- [37] B.T. Lester, T. Baxevanis, Y. Chemisky, D.C. Lagoudas, Review and perspectives: shape memory alloy composite systems, *Acta Mech.* 226 (2015) 3907–3960. doi:10.1007/s00707-015-1433-0.

- [38] A. Ishida, Ti–Ni–Cu/polyimide composite-film actuator and simulation tool, *Sensors Actuators A Phys.* 222 (2015) 228–236. doi:10.1016/j.sna.2014.12.012.
- [39] A. Ishida, M. Sato, Ti-Ni-Cu shape-memory alloy thin film formed on polyimide substrate, *Thin Solid Films.* 516 (2008) 7836–7839. doi:10.1016/j.tsf.2008.04.091.
- [40] A. Ishida, M. Sato, Development of Polyimide/SMA Thin-Film Actuator, *Mater. Sci. Forum.* 654–656 (2010) 2075–2078. doi:10.4028/www.scientific.net/MSF.654-656.2075.
- [41] A. Ishida, V. Martynov, Sputter-Deposited Alloy Thin Films : Properties and Applications, *MRS Bull.* (2002) 111–114.
- [42] V.G. Kotnur, F.D. Tichelaar, W.T. Fu, J.T.M. De Hosson, G.C.. A.M. Janssen, Shape memory NiTi thin films deposited at low temperature, *Surf. Coatings Technol.* 258 (2014) 1145–1151. doi:10.1016/S0921-5093(99)00403-7.
- [43] V.G. Kotnur, F.D. Tichelaar, G.C. a M. Janssen, Sputter deposited Ni-Ti thin films on polyimide substrate, *Surf. Coatings Technol.* 222 (2013) 44–47. doi:10.1016/j.surfcoat.2013.01.058.
- [44] K. Akash, S.S. Mani Prabu, S. Ashish, T. Tameshwer Nath, S. Karthick, I.A. Palani, Investigations on the Life cycle Behavior of Cu-Al-Ni/Polyimide Shape Memory Alloy Bi-morph at Varying Substrate Thickness and Actuation conditions, *Sensors Actuators A Phys.* (2016). doi:10.1016/j.sna.2016.12.008.
- [45] R. Dasgupta, A.K. Jain, P. Kumar, S. Hussein, A. Pandey, Effect of alloying constituents on the martensitic phase formation in some Cu-based SMAs, *J. Mater. Res. Technol.* 3 (2014) 264–273. doi:10.1016/j.jmrt.2014.06.004.
- [46] M. Gojić, L. Vrsalović, S. Kožuh, A. Kneissl, I. Anžel, S. Gudić, B. Kosec, M. Kliškić, Electrochemical and microstructural study of Cu-Al-Ni shape memory alloy, *J. Alloys Compd.* 509 (2011) 9782–9790. doi:10.1016/j.jallcom.2011.07.107.
- [47] I. Shishkovsky, I. Yadroitsev, Y. Morozov, Laser-assisted synthesis in Cu-Al-Ni system and some of its properties, *J. Alloys Compd.* 658 (2016) 875–879. doi:10.1016/j.jallcom.2015.10.299.
- [48] L. Sun, W.M. Huang, Z. Ding, Y. Zhao, C.C. Wang, H. Purnawali, C. Tang, Stimulus-responsive shape memory materials: A review, *Mater. Des.* 33 (2012) 577–640. doi:10.1016/j.matdes.2011.04.065.
- [49] C. Espinoza Torres, a. M. Condó, N. Haberkorn, E. Zelaya, D. Schryvers,

- J. Guimpel, F.C. Lovey, Structures in textured Cu–Al–Ni shape memory thin films grown by sputtering, *Mater. Charact.* 96 (2014) 256–262. doi:10.1016/j.matchar.2014.08.005.
- [50] E.M. Mazzer, C.S. Kiminami, C. Bolfarini, R.D. Cava, W.J. Botta, P. Gargarella, Thermodynamic analysis of the effect of annealing on the thermal stability of a Cu–Al–Ni–Mn shape memory alloy, *Thermochim. Acta.* 608 (2015) 1–6. doi:10.1016/j.tca.2015.03.024.
- [51] M. Izadinia, K. Dehghani, Structure and properties of nanostructured Cu-13.2Al-5.1Ni shape memory alloy produced by melt spinning, *Trans. Nonferrous Met. Soc. China.* 21 (2011) 2037–2043. doi:10.1016/S1003-6326(11)60969-2.
- [52] Z. Li, Z.Y. Pan, N. Tang, Y.B. Jiang, N. Liu, M. Fang, F. Zheng, Cu–Al–Ni–Mn shape memory alloy processed by mechanical alloying and powder metallurgy, *Mater. Sci. Eng. A.* 417 (2006) 225–229. doi:10.1016/j.msea.2005.10.051.
- [53] Z.M. Pakhuruddin, K. Ibrahim, A. Abdul, Azlan, Properties of polyimide substrate for applications in flexible solar cells, *Optoelectron. Adv. Mater.* 7 (2013).
- [54] Q. Meng, J. Hu, A review of shape memory polymer composites and blends, *Compos. Part A Appl. Sci. Manuf.* 40 (2009) 1661–1672. doi:10.1016/j.compositesa.2009.08.011.
- [55] K. Akash, K. Chandan, G. Parikshit, N.D. C, R. Disawal, B.K. Lad, V. Singh, I.A. Palani, Investigations on Transformer Oil Temperature Sensing using CuAlNi / Polyimide Shape Memory Alloy composite film, in: *Behav. Mech. Multifunct. Mater. Compos.* 2017, SPIE Proceedings, 2017: pp. 1–6. doi:10.1117/12.2259898.